

**Corrosion Rate Monitoring Using  
PCB-based Multielectrodes Array Sensors**

By

**Mohamad Faiz Bin Shafie**

**Dissertation**

submitted in partial fulfillment of  
the requirements for the  
**Bachelor of Engineering (Hons)**  
**(Electrical & Electronics Engineering)**

**May 2011**

**Universiti Teknologi PETRONAS**

**Bandar Seri Iskandar**

**31750 Tronoh**

**Perak Darul Ridzuan**

# **CERTIFICATION OF APPROVAL**

## **Corrosion Rate Monitoring Using PCB-based Multielectrodes Array Sensors**

By

**Mohamad Faiz Bin Shafie**

A project dissertation submitted to  
Electrical and Electronics Engineering Programme  
Universiti Teknologi PETRONAS  
in partial fulfillment of the requirements for the  
BACHELOR OF ENGINEERING (Hons)  
(ELECTRICAL AND ELECTRONICS ENGINEERING)

Approved:

---

Dr. Zainal Arif bin Burhanudin

Project Supervisor

Universiti Teknologi PETRONAS

TRONOH, PERAK.

MAY 2011

## **CERTIFICATION OF ORIGINALITY**

This is to certify that I am responsible for the work submitted in this project, that the original work is my own except as specified in the references and acknowledgements, and that the original work contained herein have not been undertaken or done by unspecified sources or persons.



---

**MOHAMAD FAIZ BIN SHAFIE**

## ABSTRACT

Corrosion is a natural process occurs due to the electrochemical process that may affect the human life, unscheduled shutdowns, and environmental contamination. Thus, the efficient corrosion monitoring and inspection techniques are important to control the effect of corrosion. The purpose of this project is to develop automated corrosion rate monitoring system using PCB-based multi electrodes array sensor (MAS). The automated switching circuit will communicate with the Keithley 6487 Picoammeter to measure the  $I_{corr}$  ( $I_{corr}$ ) when the MAS is immersed in the corrosive environment. The real time corrosion rate will be captured using the data acquisition system and the data will be analyzed. The automated switching circuit is being fabricated in Printed Circuit Board (PCB) consist of microcontroller, relays 5VDC, transistors and resistors. The communication between excelINX for Keithley 6487 Picoammeter and microcontroller were also attempted. However, due to time constrain it is left for future work. Maximum corrosion rate monitoring using PCB-based MAS experiment was done. First experiment use 3%wt, 6%wt and 9%wt sea salt solution to observe the capabilities of PCB-based MAS in detecting the changes of solution concentration. Second experiment is to determine the effect of conformal coating on PCB-based MAS performance. The corrosion recognized capability is tested in acidic (HCl) solution with concentration 0.5Mol and 2Mol using cyanoacrylate and epoxy conformal coating. PCB-based MAS can detect the changes of solution concentration and cyanoacrylate conformal coating on copper produce low maximum corrosion rate compare to the epoxy because of the inhibiting property that it have. In addition, peeling off epoxy affected the maximum corrosion rate when immersed in HCl.

## **ACKNOWLEDGEMENT**

Assalamualaikum. Firstly, I would like to express my gratitude to Allah S.W.T that gives me chance for me to explore and gain knowledge about His portion of knowledges. He gave me strength and health to finish my Final Year Project along this whole year (July 2010-May 2011). Alhamdulillah. Praise to Allah. Not forgotten to my family, along this project progress, I did not have much time to be with my family. Thank you for your support and understanding. Besides, I would like to thanks my supervisor, Dr. Zainal Arif bin Burhanudin who is really committed in his research work, sharing his thought, experiences and advices about the research in corrosion monitoring system which is really new to me. Aysha Salman, who is the PhD student that previously doing the same project for her Master in Science, thank you for your knowledges and advices that you share to me about this project. In addition, thanks to the technicians of Electrical & Electronics Department that share their knowledges and time in designing until finish fabricating the Printed Circuit Board External Switching Circuit and PCB-based Multielectrodes Array Sensors. To all my friends Electrical & Electronics students (July 2006) that helping me in various ways to complete this project, I really thank for your time sacrifices to help me design the circuit on Bread board, Vera board and PCB board yet try to troubleshooting the problem that occur on the first PCB board. Without your supports and help, I am sure that this project is not going to end successfully. Thank you very much.

## TABLE OF CONTENTS

<b>ABSTRACT</b> .....	iv
<b>ACKNOWLEDGEMENT</b> .....	v
<b>LIST OF TABLES</b> .....	x
<b>LIST OF FIGURES</b> .....	xiv
<b>LIST OF ABBREVIATIONS</b> .....	xii
<b>CHAPTER 1 INTRODUCTION</b> .....	1
1.1 Background of Study.....	1
1.2 Problem Statement.....	2
1.3 Objective.....	2
1.4 Scope of Study.....	2
1.4.1 Understand the corrosion process.....	2
1.4.2 Schematic and board layout of PCB-based MAS design.....	2
1.4.3 Switching circuit design.....	3
1.4.4 Communication between microcontroller and exceLINX Software.....	3
1.4.5 Experimental procedures and data analysis.....	3

<b>CHAPTER 2 LITERATURE REVIEW.....</b>	<b>4</b>
2.1 Corrosion Phenomenon.....	4
2.2 Types of Corrosion.....	5
2.3 Corrosion Monitoring.....	6
2.4 Corrosion Monitoring Techniques.....	7
2.4.1 Physical Monitoring Techniques.....	8
2.4.2 Electrochemical Monitoring Techniques.....	10
2.5 Maximum Localized Corrosion Rate Equation and Parameter..	12
<b>CHAPTER 3 METHODOLOGY.....</b>	<b>14</b>
3.1 Procedure Identification.....	14
3.2 Fundamental of Corrosion Measurement Technique.....	15
3.3 Concept of Switching Technique.....	18
3.4 Communication between Microcontroller and PC.....	20
3.5 Experimental Setup.....	22
3.5.1 First experimental setup.....	23
3.5.2 Second experimental setup.....	24
3.6 Tools and Equipments.....	24

<b>CHAPTER 4 RESULT AND DISCUSSION.....</b>	<b>25</b>
4.1 Design, Characterization and Fabrication of Planar PCB- Based MAS.....	25
4.2 Switching Circuit.....	29
4.3 Corrosion detection capabilities on PCB-based MAS.....	34
4.3.1 First experiment.....	34
4.3.1.1 Cyanoacrylate Coating PCB-based MAS in Sea Salt Solution.....	34
4.3.1.2 Epoxy Coating PCB-based MAS in Sea Salt Solution.....	37
4.3.2 Second experiment.....	41
4.3.2.1 Cyanoacrylate Conformal Coating in HCl.....	41
4.3.2.2 Epoxy Conformal Coating in HCl.....	43
4.3.3 Comparison of two conformal coating.....	46
4.3.4 Comparison PCB-based MAS and EIS Maximum Corrosion Rates.....	47



<b>CHAPTER 5 CONCLUSION AND RECOMMENDATION.....</b>	<b>48</b>
5.1 Conclusion.....	48
5.2 Recommendation.....	49
 <b>REFERENCES.....</b>	 <b>50</b>
 <b>APPENDICES.....</b>	 <b>52</b>

## **LIST OF TABLES**

**Table 1: Board Layout Description**

**Table 2: List of Tools and Equipments**

**Table 3: Simulation Circuit's Data**

**Table 4: Circuit Testing's Data**

**Table 5: Comparison of PCB-based MAS and EIS copper maximum corrosion rates.**

## LIST OF FIGURES

Figure 1: Corrosion phenomenon.....	5
Figure 2: Typical cross sectional shape of corrosion pits.....	6
Figure 3: The localized corrosion of metal: current between anode and cathode flow within the metal surface.....	11
Figure 4: Flowchart of the FYP 1 and FYP 2.....	14
Figure 5: Maximum corrosion rate measurement schematic.....	15
Figure 6: Schematic for measuring current $I_1$ .....	19
Figure 7: Schematic for measuring current $I_2$ .....	19
Figure 8: Communication methods.....	20
Figure 9: System Overview.....	21
Figure 10: Board Layout of USB to UART Converter.....	21
Figure 11: ExcelINX software to control measurement during experiment....	22
Figure 12: Experimental Measurement setup.....	22
Figure 13: Microcontroller.....	24
Figure 14: Relays.....	24
Figure 15: Schematic layout for the PCB-based MAS.....	26
Figure 16: Design of Board layout for the PCB-based MAS.....	26
Figure 17: Flowchart of PCB fabrication.....	27

Figure 18:UV Film for PCB and Fabricated PCB based Multielectrode Array Sensors.....	28
Figure 19: Switching circuit using microcontroller, relays and transistors.....	29
Figure 20: Example of the switching circuit (only 3 electrodes).....	30
Figure 21: Circuit testing.....	32
Figure 22: Board Layout of the PCB external circuit.....	33
Figure 23: Real external circuit.....	33
Figure 24: Corrosion current measured for cyanoacrylate conformal coating in sea salt solution.....	35
Figure 25: Anodic current for cyanoacrylate conformal coating in sea salt solution.....	36
Figure 26: Maximum corrosion rate using high anodic current for cyanoacrylate conformal coating in sea salt solution. ....	36
Figure 27: Corrosion current measured for epoxy conformal coating in sea salt solution.....	38
Figure 28: Anodic current for epoxy conformal coating in sea salt solution....	38
Figure 29: Maximum corrosion rate using high anodic current for epoxy conformal coating in sea salt solution.....	39
Figure 30: Maximum Localized Corrosion Rate and Maximum Localized Depth for Cu in Sea Salt Solution.....	40
Figure 31: Corrosion current measured for cyanoacrylate conformal coating in HCl.....	42
Figure 32: Anodic current for cyanoacrylate conformal coating in HCl.....	42

Figure 33: Maximum corrosion rate using high anodic current for cyanoacrylate conformal coating in HCl.....43

Figure 34: Corrosion current measured for epoxy conformal coating in HCl...44

Figure 35: Anodic current for epoxy conformal coating in HCl.....44

Figure 36: Maximum corrosion rate using high anodic current for epoxy conformal coating in HCl.....45

Figure 37: Comparison maximum corrosion rate for two conformal coating PCB-based MAS in HCl solution.....45

## LIST OF ABBREVIATIONS

<b>PCB</b>	Printed Circuit Board
<b>MAS</b>	Multi Electrodes Array Sensor
<b><math>I_{\text{corr}}</math></b>	Corrosion Current
<b><i>ER</i></b>	Electrical Resistance
<b>LPR</b>	Linear Polarization Resistance
<b>EN</b>	Electrochemical Noise
<b>EPN</b>	Electrochemical Potential Noise
<b>ECN</b>	Electrochemical Current Noise
<b><math>R_n</math></b>	Noise Resistance
<b>CMAS</b>	Coupled Multielectrode Array Sensors
<b>GPIB</b>	General Purpose Interface Bus
<b><u>Cu</u></b>	<u>Copper</u>
<b>LED</b>	Light Emitting Diode
<b>PC</b>	Personal Computer
<b>CR<sub>max</sub></b>	Maximum Corrosion Rate
<b><math>I^{\text{a}}_{\text{max}}</math></b>	Maximum Anodic Current
<b>HCl</b>	Hydrochloric Acid

# CHAPTER 1

## INTRODUCTION

### 1.1 Background of Study

Corrosion is a nature phenomenon regarding the degradation of the materials such as metal and polymer. Metal degradation is an electrochemical process which involves the oxidation of the metals. There are two types of corrosion; uniform corrosion and localized corrosion.

Uniform corrosion is the attack of a metal at essentially the same at all exposed areas of its surface. At no point is the penetration of the metal by corrosion twice as great as the average rate [1]. Uniform attack is detectable and its effects are predictable thus it will less trouble compared to the unseen corrosion.

Localized corrosion can be described as corrosion occurring at one part of a metal surface at higher rate over the rest of the surface [2].It is also known by the cavities or holes are produces in the material. This type of corrosion is more dangerous because it is difficult to identify and predict the effect. A small, narrow pit with minimal overall metal loss can lead to the failure of an engineering system [3].

Corrosion in oil and gas industry especially the internal corrosion of pipelines and others hidden components are a matter of concern for many engineers and scientists because it relates to the loss in economical or even human life.

## **1.2 Problem Statement**

Multielectrode array sensors is a technique that have ability to detect and monitor localized corrosion under numerous corrosive environment. It also can be part of any monitoring system to continuously monitor either internal or external localized corrosion.

Previously, corrosion monitoring using PCB-based multielectrodes array sensor using manually switching on the breadboard to decoupled one electrode from another nine electrodes. Thus the measurements of  $I_{\text{corr}}$  will take longer time to and it will be not efficient. Thus, automated maximum corrosion rate monitoring system need to be implement to enhance the measurement, corrosion monitoring and data analysis.

## **1.3 Objective**

The objective of this project is to create an automated measurement technique for determining the corrosion current ( $I_{\text{corr}}$ ); by introducing automated switching circuit.

## **1.4 Scope of Study**

### *1.4.1 Understand the corrosion process*

Understand the chemical process of corrosion, corrosion monitoring system technologies that has been vital nowadays.

### *1.4.2 Schematic and board layout of PCB-based MAS design.*

Eagle software 5.6.0 is used to design the schematic and board layout for PCB-based MAS.



#### *1.4.3 Switching circuit design*

Assembly language programming is used to program switch circuitry in the PIC 16F877A or PIC 18FXXX. Design a switching circuit using the PIC-based to control the relays as the switches connected to the PCB-based multielectrode array sensors. The circuit perhaps will be build in the PCB as the finalize circuit, in veroboard and breadboard as the testing functionality of the board.

#### *1.4.4 Communication between microcontroller and exceLINX Software*

The microcontroller PIC 16F877A or PIC 18FXXX needs to be programmed so that it can be communicated with the Keithley 6487 Picoammeter Software which is exceLINX. Thoroughly, it will use USB-UART converter to communicate the PIC and computer. Visual Basic will be used to program the communication between the devices. It will trigger a signal to the software to start the data capturing when the automated switching system is turn ON.

#### *1.4.5 Experimental procedures and data analysis*

When the automated switching circuitry has finished fabricated, the maximum corrosion rate monitoring experiment will be conducted in the acidic corrosive solution. Thus all the procedures need to be understood well in order to perform the experiment.

## **CHAPTER 2**

### **LITERATURE REVIEW**

#### **2.1 Corrosion Phenomenon**

Corrosion is naturally occurring phenomenon. It occurs not only at the metal but in ceramics as well as polymers. The common term used is degradation. However, the metallic corrosion is known to have relatively more adverse effects. Thus, researchers, scientists and engineers have a very deep interest to solve the problem regarding the corrosion. This is because it can effect in economical and human loses [4]. Metallic corrosion occurs with presence from the four main elements. The elements are:

1. Anode
2. Cathode
3. Electrolyte (corrosion solution)
4. Metallic conductor

Corrosion only can happen if these four main elements are in presence. The researchers, scientists and engineers are determining to eliminate one or few of the elements to ensure that the corrosion is minimized.

When corrosion takes place, metal dissolves in the corrosive solution it will leave electron behind. These electrons moves from the corroding electrode (anode) to the less corroding electrode (cathode) producing a current called  $I_{corr}$ . If this current can be measured, then the rate at which the metal is corroding can be calculated [5].

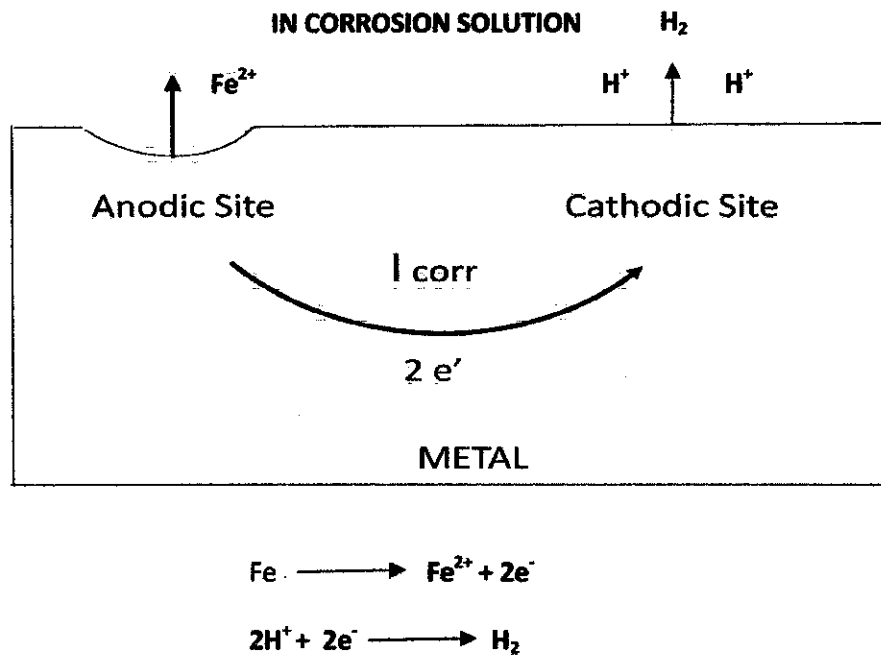


Figure 1: Corrosion phenomenon.

## 2.2 Types of Corrosion

Corrosion can lead to the failures in plant infrastructure and others especially related to the metal equipment. It is costly to repair. There are several types of corrosion such as uniform corrosion and localized corrosion.

Uniform corrosion attacks the metal surface uniformly. From corrosion inspection, the corrosion can be detectable by eyesight or other corrosion monitoring system yet the effect can be predicted. On the other hand, uniform corrosion the anodes and cathodes cannot easily being detected since the corrosion randomly emerged as a result of electrochemical process.

Localized corrosion is dangerous than uniform corrosion because it is difficult to detect, predict and design against [6]. The most common type of localized corrosion is pitting. It is more concentrated to a certain part of the metal that exposed to the corrosive surroundings. Thus, the anodes and

cathodes can clearly be spotted at the surface of the metal by using the corrosion monitoring system. Figure 2 shows the typical cross-sectional shapes of corrosion pits.

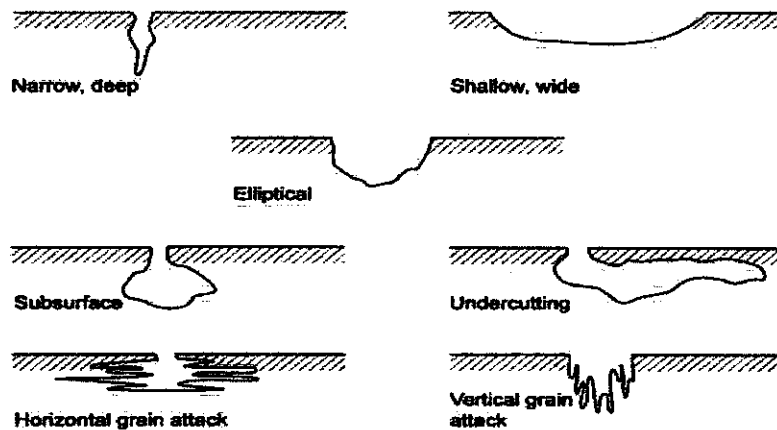


Figure 2: Typical cross-sectional shapes of corrosion pits [7].

### 2.3 Corrosion Monitoring

Corrosion monitoring refers to the corrosion measurements or acquiring data on the rate of material degradation. Corrosion monitoring is a more complex process [7]. This is because:

1. There are different types of corrosion
2. Corrosion may be uniform over an area or concentrated in a very small area.
3. General corrosion rates may vary substantially, even over relatively short distances
4. There is no single measurement technique that will detect all of those various conditions.

The application of corrosion monitoring should be presented as an investment to fulfill some objectives:

1. Improved safety
2. Production of early warning before cause serious damage
3. Reduced maintenance costs
4. Reduced pollution and contamination risk
5. Longer intervals between scheduled maintenance
6. Reduced operating costs.

## **2.4 Corrosion Monitoring Techniques**

The corrosion monitoring system can be divided into two techniques which are the direct techniques monitoring system and indirect techniques monitoring system.

Direct techniques monitoring system basically is the direct measurement of corrosion rate at the metal corroded. There are many direct techniques in corrosion monitoring which are metal loss coupons (weight loss), electrical resistance, linear polarization resistance, zero resistance ammeter, potentiodynamic- galvanodynamic polarization, electrochemical noise, electrochemical impedance spectroscopy, ultrasonic testing, and coupled multielectrode array sensors.

Indirect techniques monitoring system is a technique that measures the parameters that affect the corrosion and that being effect by corrosion. The parameters being measured such as hydrogen content, pH of metal, redox potential, total no of acid, nitrogen content, salt content, temperature, pressure, flow velocity and flow regime.

The examples of indirect monitoring techniques are hydrogen monitoring, water chemistry analysis, fluid detection, process parameter monitoring, deposition monitoring, thermography, residual inhibitor and sample chemical analysis.

In this project, the author will focus on the direct technique of corrosion monitoring system. There are two types of direct technique of corrosion monitoring systems which are physical and electrochemical monitoring system.

#### 2.4.1 *Physical Monitoring Techniques*

##### a. Weight loss method

Weight loss method is very established corrosion rate monitoring technique which compares the weight before and after (weight-loss) of the metallic coupon enter the corrosive environment. The difference in weight can determine the corrosion rate using the equation below:

$$CR = W_0 - W_1 / A \times T \quad (1)$$

In equation (1)  $W_0$  is weight of the coupon before encounter the corrosive environment,  $W_1$  is weight after corroded,  $A$  is the metal area in  $m^2$  and  $T$  is time in hour.

The limitation of this technique is it only can be used for uniform corrosion detection only and not have real time data to determine the corrosion rate.

b. Electrical resistance (ER)

ER is the other method of physical monitoring technique. As corrosion takes place and metal loss occurs, the cross sectional area of the sensing element will decrease and electrical resistance will increase. [8] The relationship is shown below in the equation (2).

$$R = \rho l/A \quad (2)$$

In equation (2),  $\rho$  is the resistivity of the metal,  $l$  is the length and  $A$  is the cross sectional area of metal. ER probe made of the same material with the corrosion rate is to be determines.

Small current applied across the metal and the resulting potential drop is measured. From the current and voltage measured, using Ohm's Law the resistance is calculated and being compared to the original non corroded probe. The difference in resistance with respect to the time is used to determine the corrosion rate. ER probes measure the metal loss directly but it only limited for the uniform corrosion rate only. The advantages are it provides real time data for corrosion rate detection, easy to use and the maintenance is low.

## 2.4.2 *Electrochemical Monitoring Techniques*

### a. Linear polarization resistance (LPR)

Linear polarization resistance (LPR) is an electrochemical based corrosion monitoring technique. An electrochemical excitation is applied to an electrode and the response of this electrode against a reference electrode is used to measure the corrosion rate. The excitation can be either voltage or current. In the case of voltage excitation a small voltage is applied to the electrode in increasing steps and the resulting response is measured. The electrode potential moves away from the corrosion potential, its polarized. The resulting is polarized of resistance,  $R_p$ . the slope of the current potential plot around the corrosion potential, Stern and Geary found that the slope is essentially linear. Thus, this technique called Linear polarization resistance. When  $R_p$  is measured, the corrosion rate can be obtained from the equation:

$$I_{\text{corr}} = B/R_p \quad (3)$$

LPR can provide the corrosion rate faster than ER, but LPR only limited to detecting the uniform corrosion only. It also needs sufficient conductive liquid for corrosion monitoring.

### b. Electrochemical noise (EN)

Electrochemical noise (EN) detects and monitors the fluctuation in potential, electrochemical potential noise (EPN) or current, electrochemical current noise (ECN) on the corroding electrode and determine the electrochemical noise resistance,  $R_n$ . EN also can identify the type of corrosion and it provides the information about the localized and pitting corrosion but the measurement is lengthy and complicated.



c. Coupled multielectrode array sensor (CMAS).

When CMAS's multiple miniature electrodes that are made from the same material undergoes corrosive environment, electrons are released from the anodic sites where the metal corrodes and travel to the cathodic sites where the metal less corrode thus produces a current flow between the these electrodes. Some of the electrodes have similar properties with the anodic sites and other has similar properties like the cathodic sites of the corroding metal. As the electrode is isolated from each other and connects with the external circuit, the electrons that are released from the anodic electrodes are forced to flow through the external circuit to the cathodic electrodes. Thus, there are anodic currents (negative) flowing into more corroding electrodes. The cathodic currents (positive) will flow out of the less corroding current [9]. This is because anode releases electrons due to metal loss (current move in the opposite direction of electron flow). This current flow produces potential drop across the resistors. This current is the determining factor in calculating the corrosion rate.

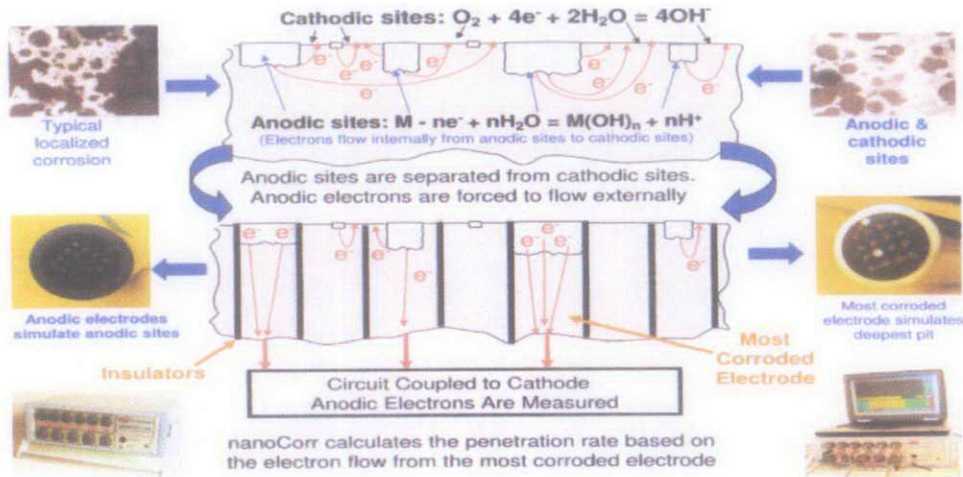


Figure 3: The localized corrosion of metal: current between anode and cathode flow within the metal surface [9].

The CMAS corrosion monitoring technique has advantage to detect and monitor localized corrosion behavior. Thus it is very useful to enhance the corrosion monitoring techniques.

## 2.5 Maximum Localized Corrosion Rate Equation and Parameters

When the anodic and cathodic are coupled, the total anodic dissolution current on the anodic currents is equal to the cathodic reduction current.

$$I_{\text{corr}} + I_{\text{in}}^{\text{c}} = I_{\text{in}}^{\text{a}} + I^{\text{c}} \quad (4)$$

Where  $I_{\text{corr}}$  is corrosion current on anodic electrode,  $I_{\text{in}}^{\text{c}}$  anodic current that flow within all the cathodes,  $I_{\text{in}}^{\text{a}}$  is the cathodic current that flows within the anode and  $I^{\text{c}}$  is the cathodic current.

On anodic electrode,  $I_{\text{corr}}$  is equal to the sum of the externally flowing anodic current and internally flowing anodic currents.

$$I_{\text{corr}} = I_{\text{ex}} + I_{\text{in}}^{\text{a}} \quad (5)$$

$I_{\text{in}}^{\text{a}}$  for the anodic electrode is smaller than  $I_{\text{ex}}$  at the coupling potential in a localized corrosion environment.

$$I_{\text{corr}} = I_{\text{ex}} \quad (6)$$

The presence of the cathodic sites on the anodic electrodes cannot be eliminated. In polarizes coupling point of CMAS, anodic current flow entirely through the external circuitry [12]. The potential through the most cathodic electrodes is measured and considered to be the highest cathodic potential among all other electrodes in CMAS. Common coupling is polarized to a potential slightly higher than the most cathodic potential. Thus, all current will flows through the external circuit. The anodic current can be expressed as in(7).

$$I_{\text{ex}} = \varepsilon I_{\text{corr}}$$

$$I_{\text{corr}} = I_{\text{ex}} / \varepsilon \quad (7)$$

$\epsilon$  is current distribution factor that represent the fractional of electrons resulting from the corrosion through the external circuit.  $\epsilon$  values varies from 0 to 1. If the electrodes is completely corroded all the current will flow through the external circuit thus the  $\epsilon$  will be close to 1. If there are some local cathodic sites, there will be internal circuit flow then  $\epsilon$  will close to 0 [5].

The maximum localized corrosion rate is in (8)

$$CR_{\max} = (1/\epsilon) I_{\max} W_e / (F\rho A) \quad (8)$$

$CR_{\max}$  is the maximum penetration rate (cm/s),  $I_{\max}$  is maximum anodic current,  $F$  is Faraday Constant (96485C/mol),  $A$  is surface area of electrode (cm<sup>2</sup>). Electrode diameter is 1.5mm thus the surface area is 0.0176 cm<sup>2</sup>,  $\rho$  is density of the electrode (g/cm<sup>3</sup>),  $W_e$  is weight (g/mol). Equivalent weight  $W_e$  is defined in [13] is given by (9):

$$W_e = \frac{1}{\sum(m_i z_i / W_i)} \quad (9)$$

Where  $m_i$  is the mass fraction,  $z_i$  is the oxidation state and  $W_i$  is the atomic weight of the component  $i$  in the electrode alloy. Since Cu is used the modified equation for  $W_e$  is in (10) [5].

$$W_e = \frac{W_c}{z_c} = 63.546 \text{ g/mol} \quad (10)$$

In addition, three standard deviations of all anodic currents in one time measurement is also calculated and used in (11) to calculate  $CR_{\max}$  for Cu. Thus, two values of  $I_{\max}$  as shown in (11) and (12) below is use to calculate  $CR_{\max}$  for Cu.

$$I_{\max}^a = 3\sigma \quad (11)$$

$$I_{\max}^a = I_{\max} \quad (12)$$

## CHAPTER 3

### METHODOLOGY

#### 3.1 Procedure Identification

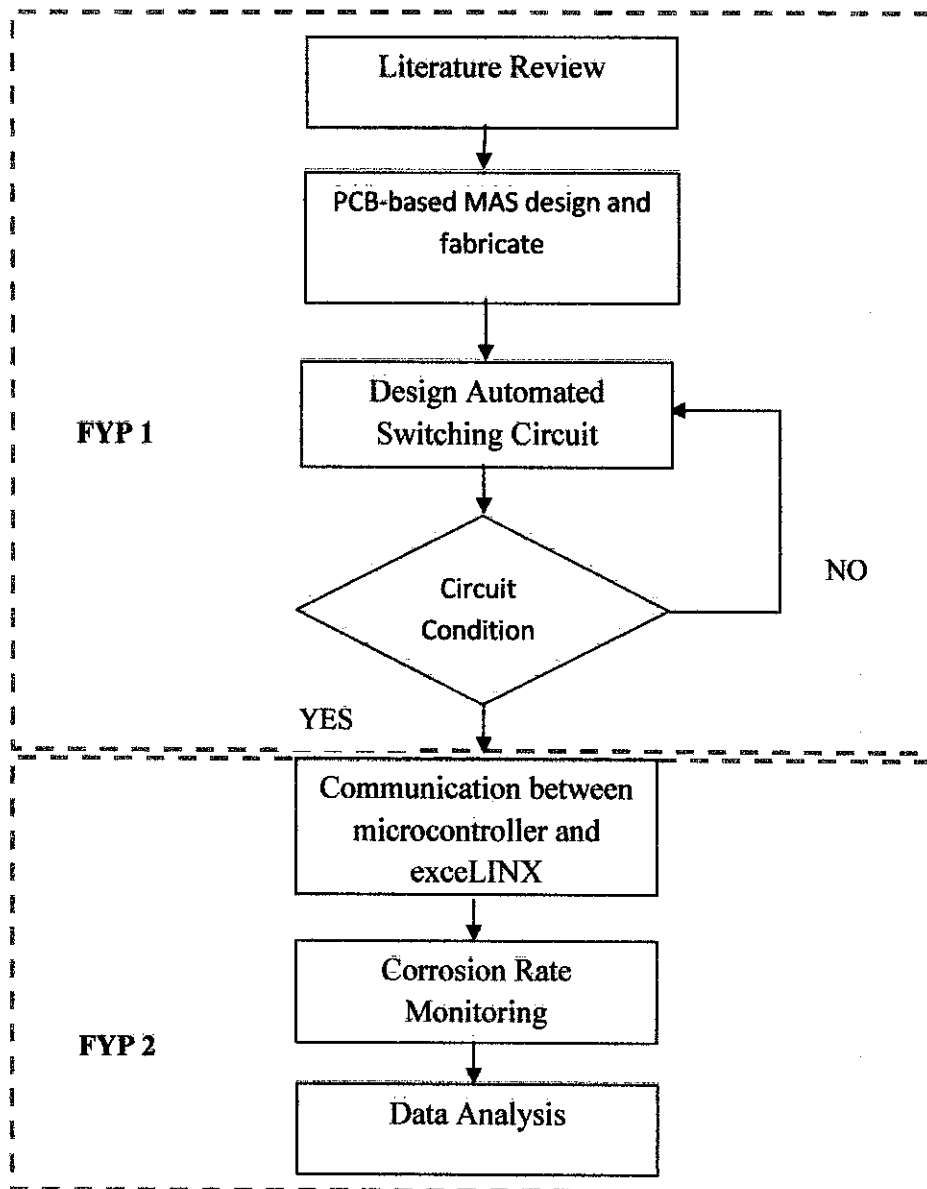


Figure 4: Flowchart of the FYP 1 and FYP 2

### 3.2 Fundamental of Corrosion Measurement Technique

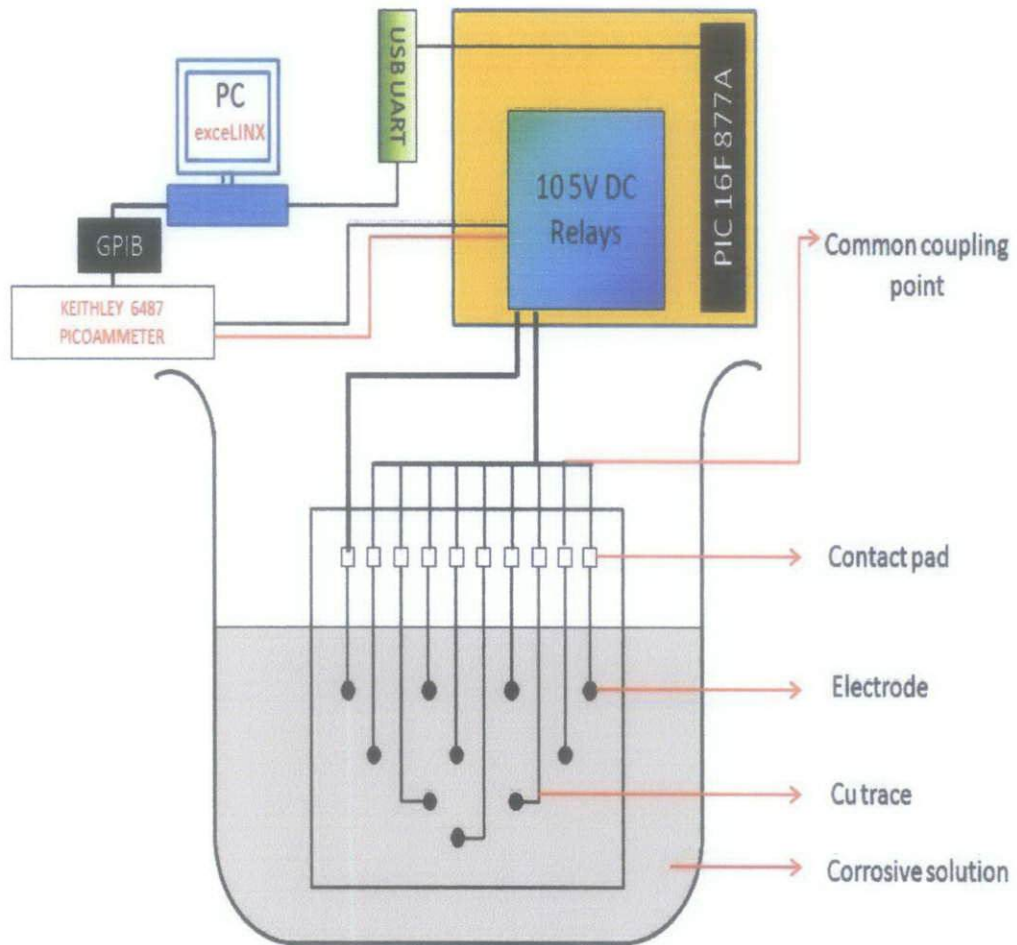


Figure 5: Corrosion rate measurement schematic

From figure 5 illustrated the fundamental of the corrosion measurement technique for the PCB-based multielectrodes array sensors.

When the sensors encounter the corrosive environment, some of the electrodes will become anodic sites and some will become cathodic sites. The electron will move from the most corrosive electrodes which are anodes site to the less corrosive electrodes that are cathodic site. Thus the current will flow between the cathodic and anodic sites in response to the electron movement. As the electrode is being decoupled from the common coupling point, the current will be forced to flow through the external circuit. Picoammeter will be connected between the decoupled electrode and the common coupling point to measure the electrode current.

Basically, the current move out from the cathodic sites into the anodic sites. Thus we can define that the anodic current is actually a negative current while cathodic current is a positive current.

Usually, when multielectrodes array sensors encounter the corrosive environment, there is an electrode which is significantly more anodic from other electrodes. It simulates the localized corroded metal piece which has highly anodic sites and surrounded by cathodic sites. This is why the anodic current from the significant anodic electrode act as parameter to determine the localized maximum corrosion rate.

The data of Icorr will be captured and transmitted using the General Purpose Interface Bus (GPIB) that will act as the communicator between instrument and the computer.

Thoroughly, when relay for electrode one decoupled from the common coupling, microprocessor will send signal through microcontroller to the USB UART. The signal from USB UART will communicate with the Visual Basic Software in the computer to trigger the ExceLINX (Keithley 6487 Picoammeter Software) to start the measurement.

Unfortunately, the ExceLINX is protected. Visual Basic for Application (VBA) coding in the exceLINX cannot be access. It is difficult to link with the coding in Visual Basic in the computer. Thus, the communication between microcontroller and computer is interrupted.

Another method to measure  $I_{corr}$  using the automated measurement is decoupling the connection from common coupling using the relays. Delays set on the microcontroller are 30 seconds because the time to finish data collection is between 8 seconds to 22 seconds. The measurement increments (the column of data collection in Microsoft Excel) in the exceLINX Scan Meter will be manually change after data being collected and before the next decoupling point occur.

### 3.3 Concept of the Switching Circuit.

A switching circuit must be designed and fabricated in order to create an automated measurement technique for determining the corrosion current, ( $I_{corr}$ ). In previous work, switching circuit built on PCB was fabricated. It use a manual switches to control the switching circuit. It is not practical because the corrosion monitoring need a long time to measure the  $I_{corr}$ . Thus, the implementation of automated measurement technique can enhance the maximum corrosion rate monitoring to the greater extent.

Switching circuit is an external circuit to force the current flow through it. Current will be measured when the electrode is decoupled from the common coupling point.

In this project, PCB- based multielectrodes array sensors have ten electrodes (electrode 1-10). Current  $I_1$  is being measured by decoupling the electrode 1 from the electrodes common coupling point. The current from the electrodes 2 until 10 will flow through the external circuit to electrode 1. All corrosion data are captured by using the picoammeter. The data are sent to the computer to be stored and analyzed. Thus the procedures remain the same to measure current  $I_2$  until  $I_{10}$ .

The concept of switching circuit is as the figure 6 and 7 below.



Measurement of  $I_1$  is done by decoupling the electrode one from the common coupling point and it is connected to the picoammeter.

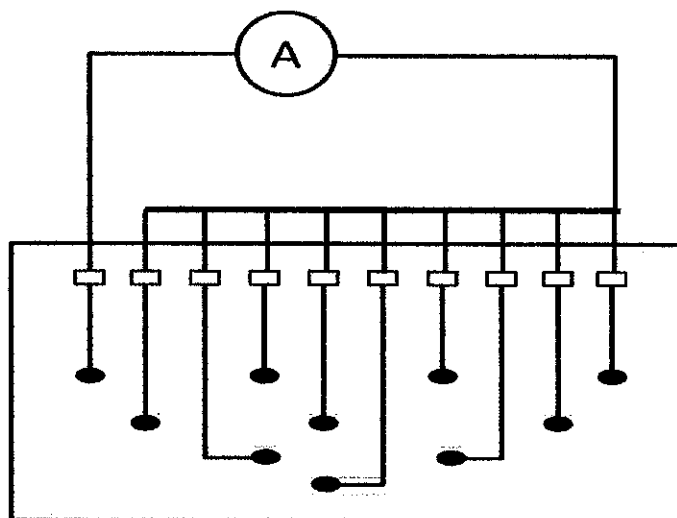


Figure 6: Schematic for measuring current  $I_1$

Measurement of  $I_2$  is done by decoupling the electrode two from the common coupling point and it is connected to the picoammeter.

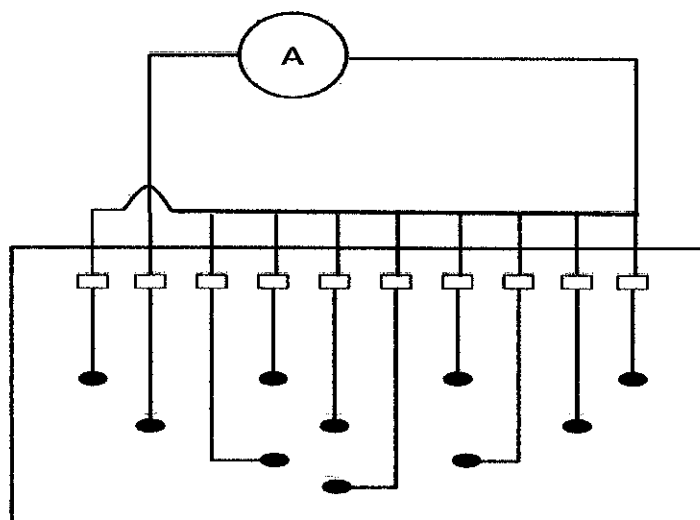
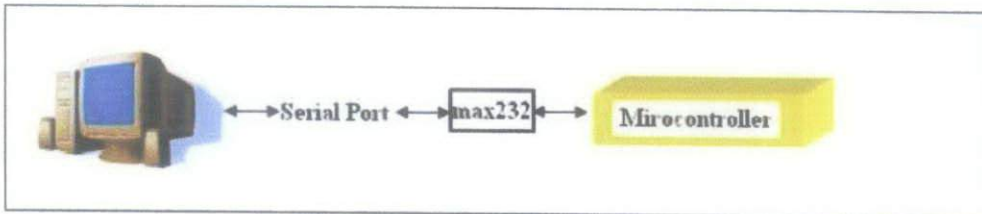


Figure 7: Schematic for measuring current  $I_2$

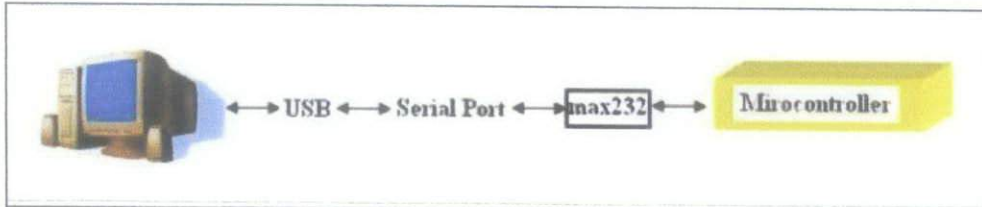
### 3.4 Communication between Microcontroller and PC

Serial communication is most popular interface between device and this applies to microcontroller and computer. UART is one of those serial interfaces. Classically, most serial interface from microcontroller to the computer is done by serial port. However, since computer serial port used RS232 protocol and microcontroller used TTL UART, a level shifter is needed between these interfaces. Recently, serial port have been phase out, it have been replaced with USB. Thus, USB to UART converter is the best device to be used in order to have direct interface between PC and microcontroller.

#### Traditional Method



(a) PC (Serial Port)



(b) PC (USB)

#### Using UC00A Method

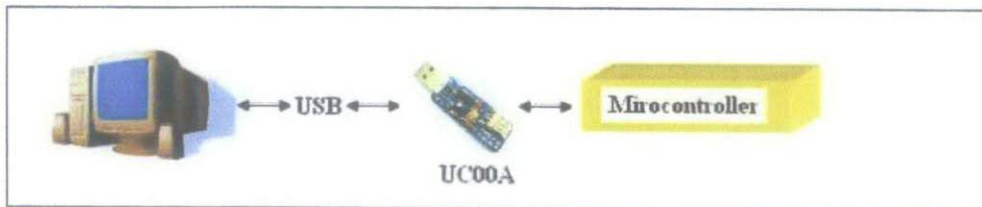


Figure 8: Communication methods [15].

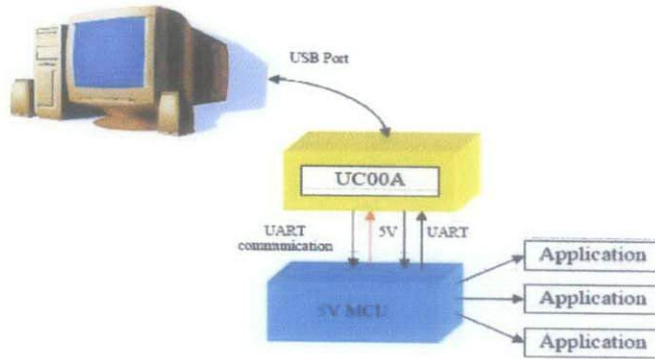


Figure 9: System Overview [15].

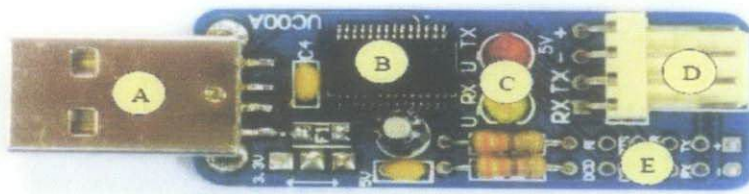


Figure 10: Board Layout of USB to UART Converter [15].

Table 1: Board Layout Description

Label	Function
A	SB A type (male)
B	USB to UART chip
C	Two LED indicator for USB's transmitter and receiver status
D	4 ways header pins for interface to microcontroller <ul style="list-style-type: none"> <li>• Pin 1 is + 5V Power Output from USB</li> <li>• Pin 2 is - (Grounding)</li> <li>• Pin 3 is TX (Transmit Pin-Device receiver pin)</li> <li>• Pin 4 is RX (UART Receive Pin-Device transmitter pin)</li> </ul>
E	2x5 extension pad for extra COM Port Feature

### 3.5 Experimental Setup

Keithley 6487 Picoammeter is the data acquisition to measure the  $I_{corr}$  during the experiment. This picoammeter configured with the computer using GPIB cable. Software exceLINX is the special build software for Keithley Picoammeter to control configuration between data acquisition, start measurement and data collection. This software is an Add-in to Microsoft Excel. Thus, all the measurement data will be stored in the selected sheet in Excel. In this exceLINX, there are two tabs which are Configure Meter and Scan Meter. Configure Meter need to be selected first in order to configure the communication between the computer and picoammeter. When configuration success, it will appear "Task stopped successfully". Next step is to open the Scan Meter which provide the user all experiment option such as how many readings per experiment, which sheet, row and column in Microsoft Excel to store the data and start measurement button. Red wire from the data acquisition will be connect to the decoupling point and black wire will be connected to common coupling wire. Ten readings will be captured for each of the electrodes. Only anodic current will be consider to be analyze using all equations in the Section 2.5.

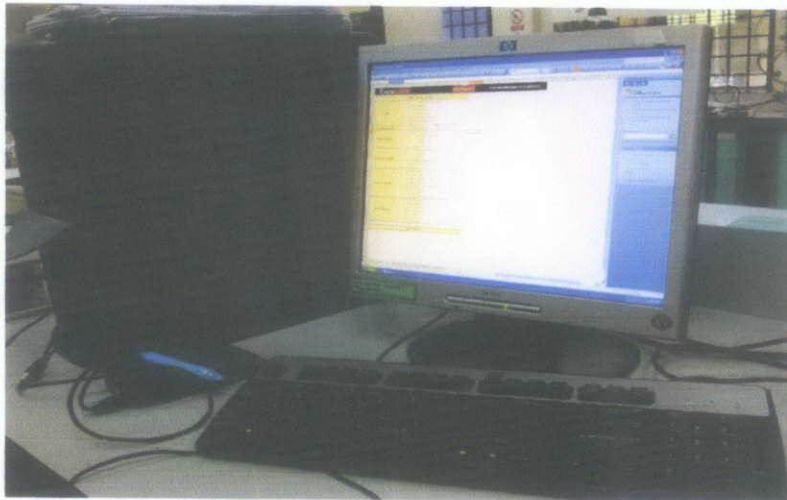


Figure 11: ExceLINX software to control measurement during experiment

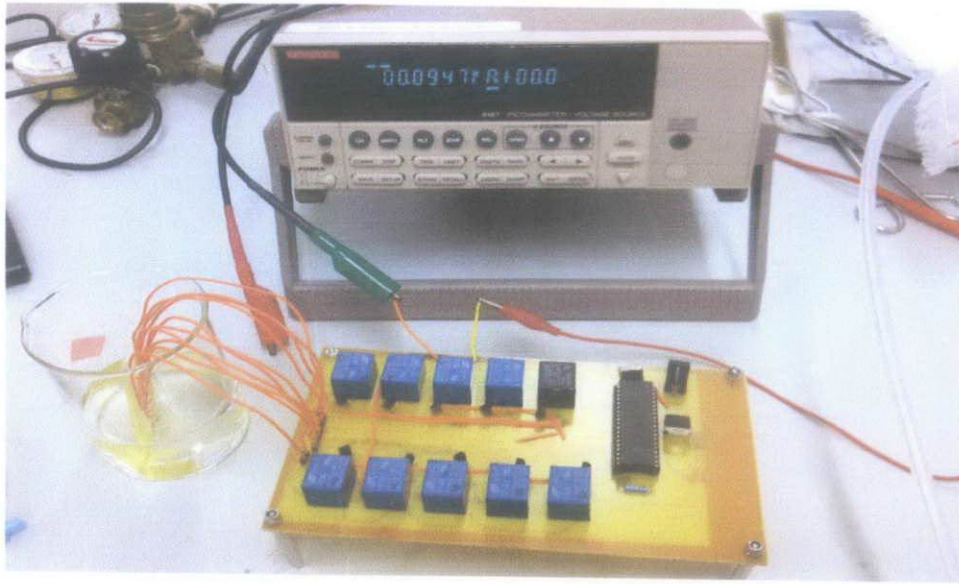


Figure 12: Experimental Measurement setup

### 3.5.1 First experimental setup.

The objective of first experiment is to observe the corrosion recognition capability of the PCB-based MAS. PCB-based MAS will be immersed in the 3%wt of sea salt solution. The solution was prepared using 3gram of sea salt added in 100ml of deionized water and stirred. Before immersed the PCB-based MAS in the solution, copper traces of PCB-based MAS were covered with cyanoacrylate or epoxy as conformal coating to protect them from environmental effects. Besides, copper electrodes on the sensor was polished using sand paper to remove the oxide layer on it. This will ensure that the electrodes corroded actively in the solution. The Keithley 6487 Picoammeter was connected to the decoupling point and common coupling point of the external circuit. 10 measurements of  $I_{corr}$  per electrodes were taken in 10 days. The result of 3%wt sea salt solution will be compare to the result of CMAS probe monitored the Cu maximum corrosion rate. Sea salt solution will be changed on day 6 from 3%wt to 6%w and 9%wt to monitor the capability of PCB-based MAS to recognize the changes environment.

### 3.5.2 Second experimental setup.

The objective of this experiment is to determine the effect of conformal coating on PCB-based MAS performance. This experiment used cyanoacrylate and epoxy conformal coating as the protection to the copper traces on the sensors from environmental effects. The corrosion recognized capability is tested in acidic (HCl) solution with concentration 0.5Mol and 2Mol.

### 3.6 Tools and equipments

Table 2: List of Tools and Equipments

Tools	Softwares
a. Relays 5VDC	a. MPLab IDE V8.56
b. Transistors 2N222	b. ISIS Professional 7
c. Microprocessor PIC 16F877A	c. PIC Simulator
d. Keithley 6487 Picoammeter	d. exceLINX
e. GPIB Card and USB UART	e. Eagle 5.6.0
f. PCB Board	f. Visual Basic



Figure 13: Microcontroller

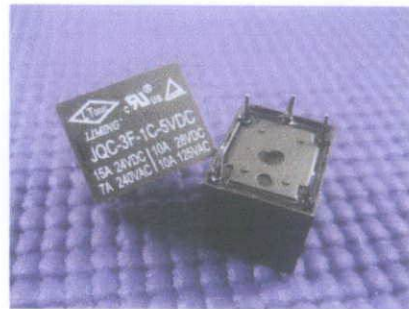


Figure 14: Relay 5VDC

## **CHAPTER 4**

### **RESULT AND DISCUSSION**

#### **4.1 Design, Characterization and Fabrication of Planar PCB-Based MAS**

CMAS probes typically have long metallic wires as electrodes. These wires will be coated with epoxy as insulation and exposed the cross-section of the wires to monitor the maximum corrosion rate. Eagle software 5.6.0 is used to design the schematic and board layout for PCB-based MAS.

The criterion for PCB-Based MAS was the electrode size or diameter. Since the PCB is the miniaturized version of CMAS, the electrode diameter has to be in the same range of 0.5mm to 2.0mm. In this research the size is chosen to be 1.5mm. The electrodes that are going to be used are made from copper (Cu). In CMAS path for the Icorr to the external circuit is the electrode itself, but in this planar PCB a conductive path is needed between the electrodes and the external circuit, thus the selection of Cu is a right choice because it is a good conductor. The minimum trace width (trace in the Cu path) in the PCB laboratory is 10mils (0.01 inches). Icorr is predicted to be small enough, thus the width of the trace will have no effect on the current flow. Thus, the trace chosen is 10mils.

Eagle software 5.6.0 is used to design the schematic and board layout for PCB-based MAS. This software is user friendly and widely used for designing the PCB circuit. It can be run on Windows operating system.

Figure 15 and 16 show the schematic and the board layout for the PCB based MAS.

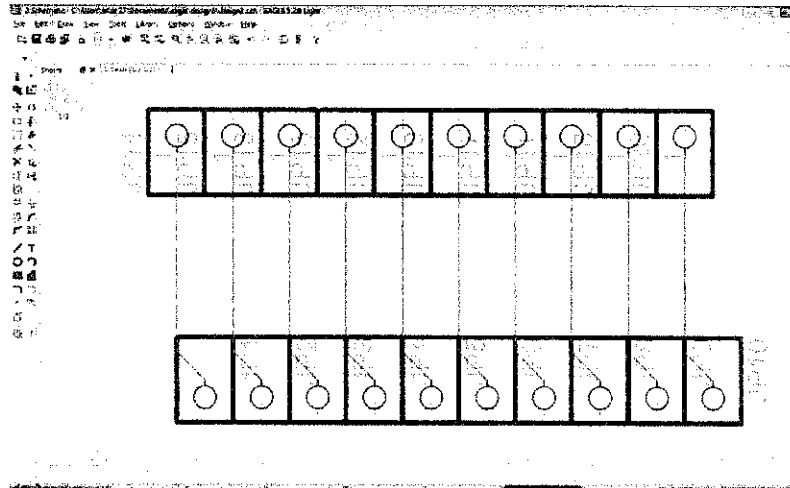


Figure 15: Schematic layout for the PCB-based MAS

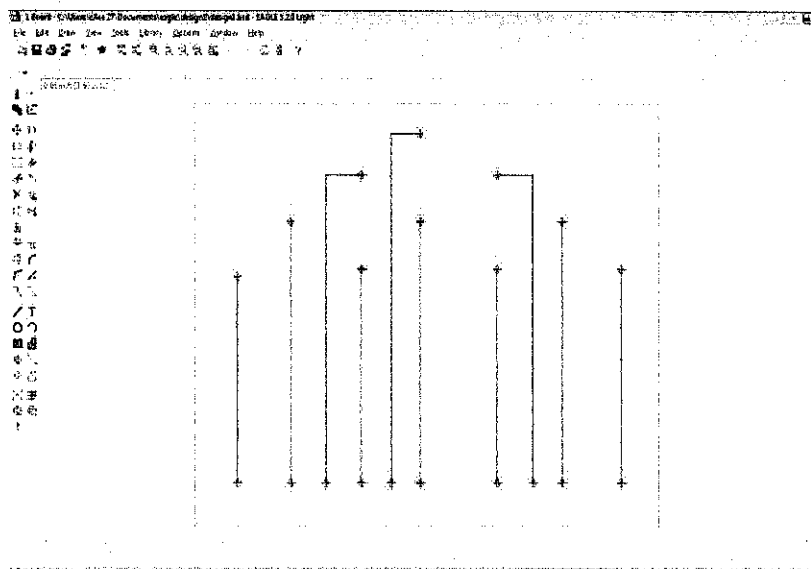


Figure 16: Design of Board layout for the PCB-based MAS



The designs in the previous page are fabricated using typical PCB process. Flowchart in figure 17 shows the PCB fabrication steps [11]:

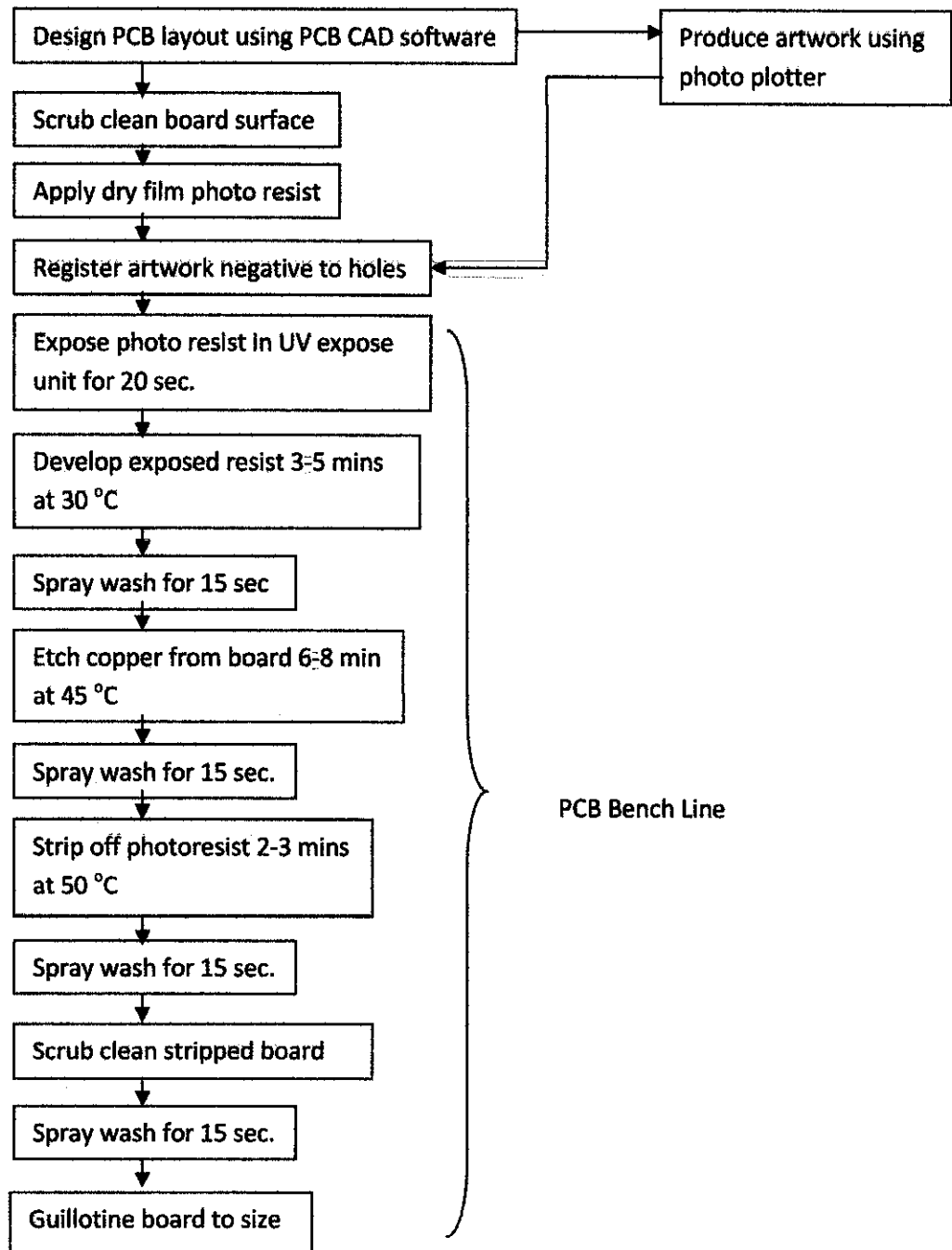


Figure 17: Flowchart of PCB fabrication

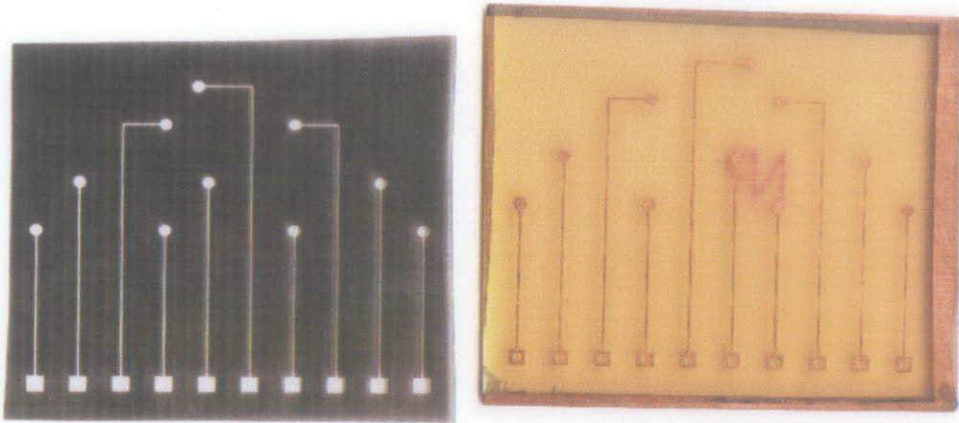


Figure 18: UV Film for PCB and Fabricated PCB-based Multielectrode Array Sensors

## 4.2 Switching Circuit

Microcontroller PIC 16F/ 18F, relays 5VDC/6VDC, transistors are used to build a set of switching circuit. After designing the circuit and programming the microcontroller, simulation is done using PIC Simulator and ISIS 7 Professional. The results of the switching circuit are shown in figure 19.

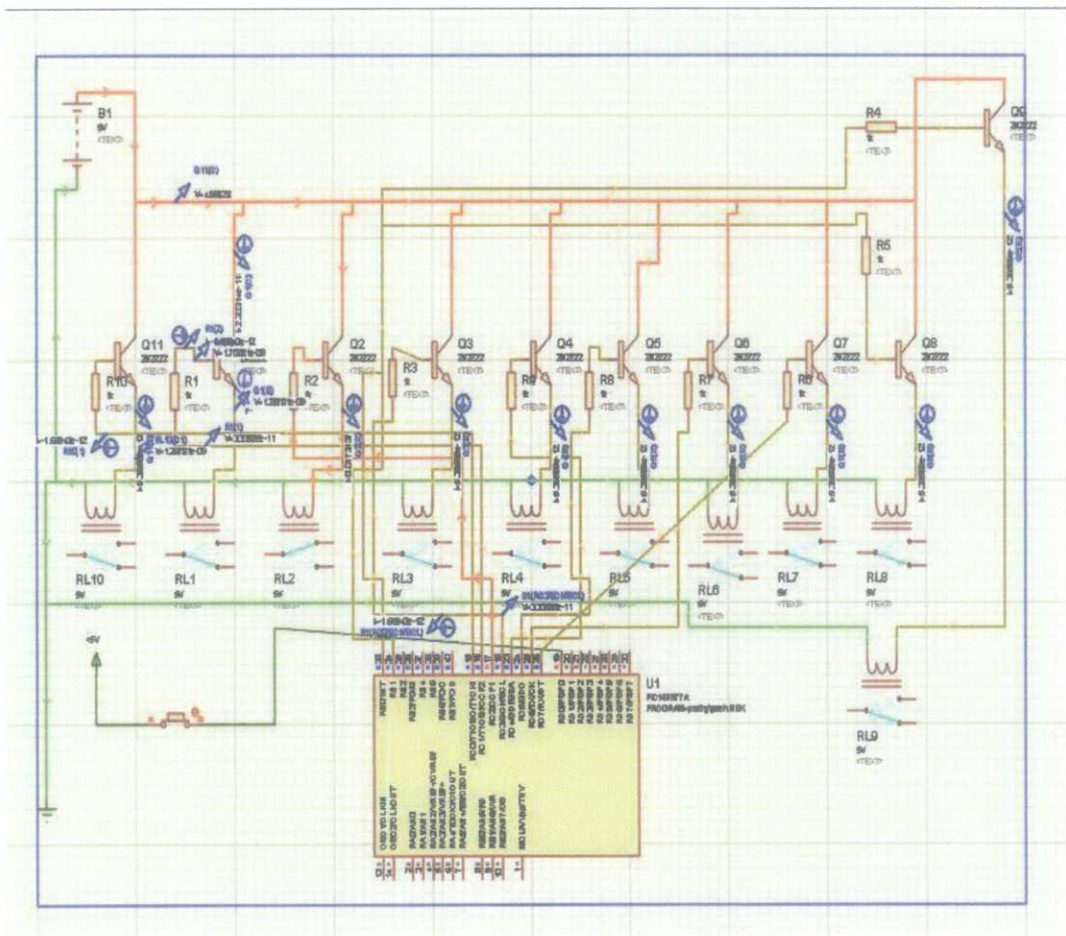


Figure 19: Switching circuit using microcontroller, relays and transistors.

From the figure 20 below, concept of switching circuit can be explained for further understanding.

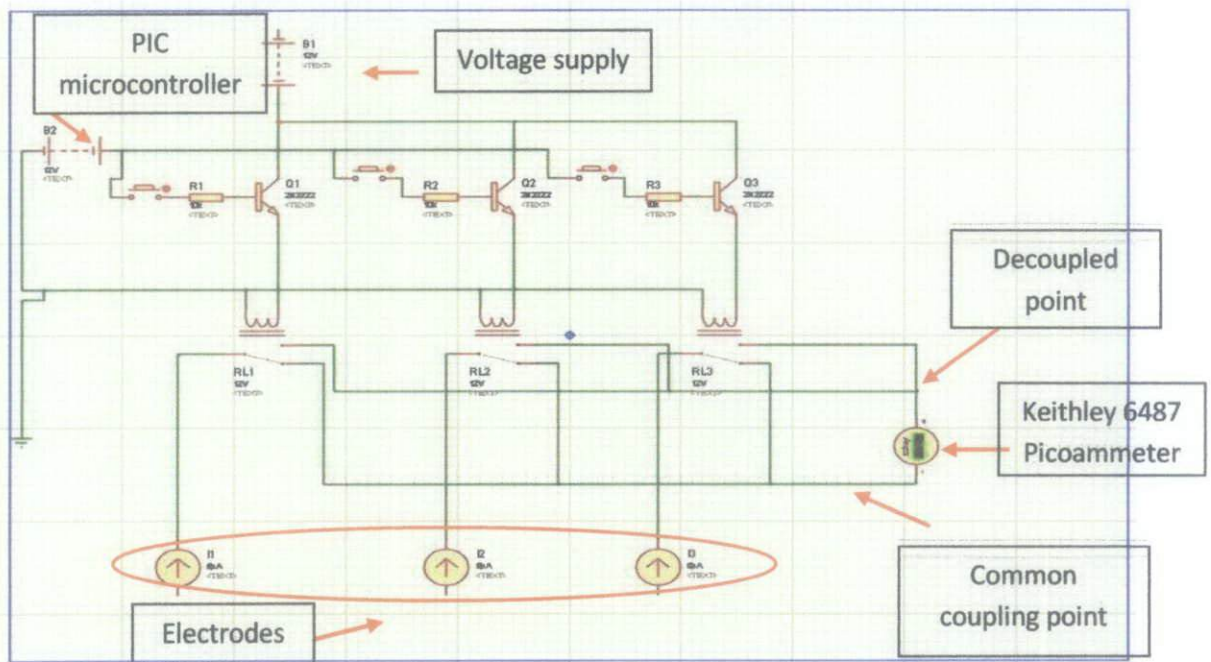


Figure 20: Example of the switching circuit (only 3 electrodes)

Voltage 5V is supplied to the microcontroller and 6V to the collector of transistors. The microcontroller basically will switch ON (5V is supplied) and will energize the respective relay. The respective relay will be connected to the decouple point while the other switches remain normally close and connected to the common coupling point. When electrode 1 decoupled, electrode 2 and 3 will couple together at the common coupling point.

Current  $I_2$  and  $I_3$  from the electrode 2 and 3 will flow to the electrode 1. Current  $I_1$  will be measured by the Keithley 6487 Picoammeter. Data for the maximum corrosion rate will be transferred to the computer and being analyzed. The maximum corrosion rate current measurement for  $I_2$  until  $I_{10}$  will use the same procedures as to measure current  $I_1$ .

From the simulation in figure 20, Table 2 below shows the values current and voltage when circuit is switch ON and OFF.

Table 3: Simulation circuit's data

<b>Value Determination Point</b>	<b>Circuit OFF Condition</b>	<b>Circuit ON Condition</b>
Voltage supply from microcontroller. V	$3.333885 \times 10^{-11}$ V	4.99797 V
Voltage supply from voltage source, V	4.99484 V	4.99484 V
Base current, $I_B$	$1.66 \times 10^{-12}$ A	0.0010158 A
Collector current, $I_C$	$2.2 \times 10^{-11}$ A	0.0172121 A
Emitter Current, $I_E$	$5.36 \times 10^{-12}$ A	0.0173136 A
Base-emitter Voltage, $V_{BE}$	$0.5 \times 10^{-9}$ V	0.74111 V

From the values in table 3, it can be explained that when circuit is in OFF condition, all the current at the collector, base and emitter of the transistor 2N222 nearly 0A. When the circuit is in ON condition, the transistor 2N222 will be biased ( $V_{BE}$  greater than 0.7V) by the voltage supplied from the microcontroller PIC 16F877A. Thus, the relays will switch ON the relays to decouple the electrodes from the common coupling point. On overall basis, as a first approximation, the base-to-emitter voltage of an operational transistor can be assumed to be 0.7V [10]. The switching circuit operated well in the simulation.

Figure 21 below shows that circuit testing using only two relays. Voltage regulator 7805 was used to regulate the power supply 9V from the battery to 5V for the operation of the microcontroller and relays. Light emitting Diode (LED) used to as an indicator to see the operational of the relays. When relays are OFF condition, the LED will OFF and when relay is ON the LED will ON. Table 3 below shows the values during the circuit testing.

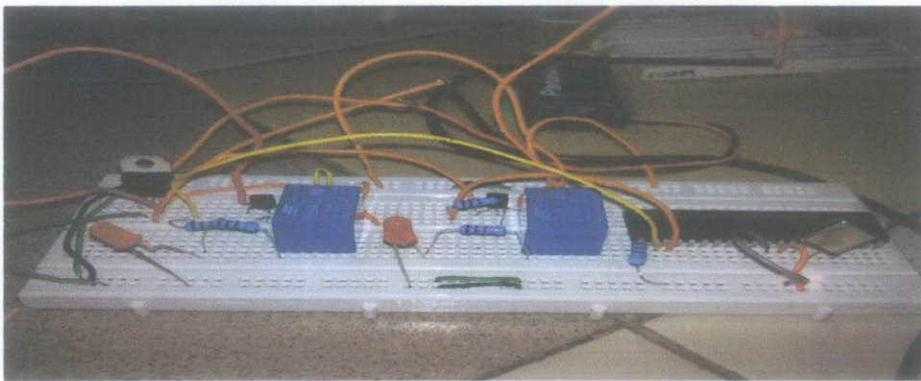


Figure 21: Circuit testing

Table 4: Circuit testing's data.

<b>Value Determination Point</b>	<b>Circuit OFF Condition</b>	<b>Circuit ON Condition</b>
Voltage supply from microcontroller. V	0 V	5 V
Voltage supply from voltage source, V	5 V	5 V
Base current, $I_B$	0 A	2mA
Base-emitter Voltage, $V_{BE}$	0 V	0.7 V

The external circuit have been designed and fabricated on the PCB board. It consist of 40 pins PIC 18F, 10 unit of relays, 10 unit of transistors, toggle switch to control the power supply, resistors to control the limit of current in circuitry, voltage regulators to regulate the supply voltage from 9V to 5V and 6V and LEDs as indicators to the power supply and relays. Figure 22 and 23 below show the board layout of the circuit and the real external circuit.

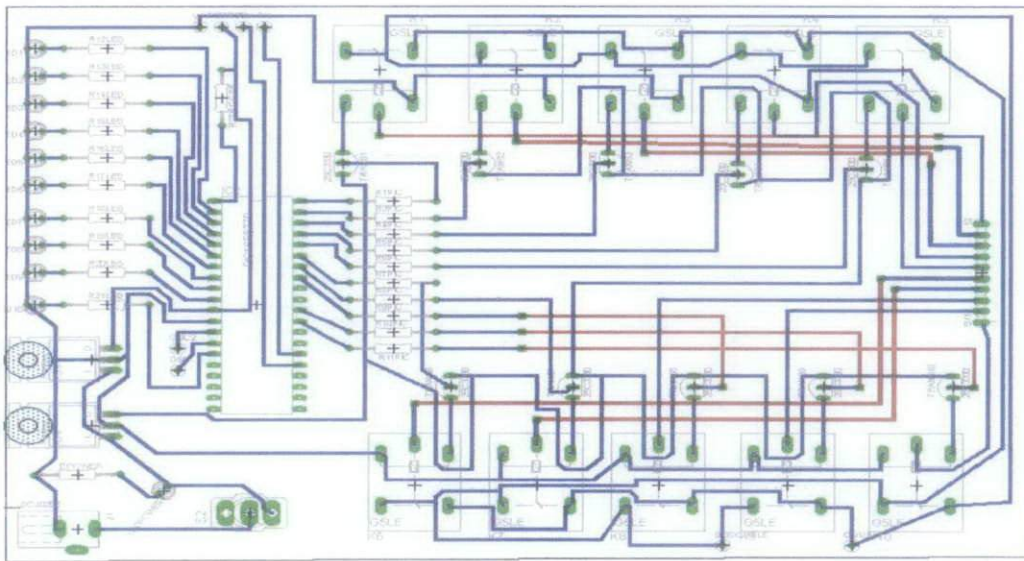


Figure 22: Board Layout of the PCB external circuit

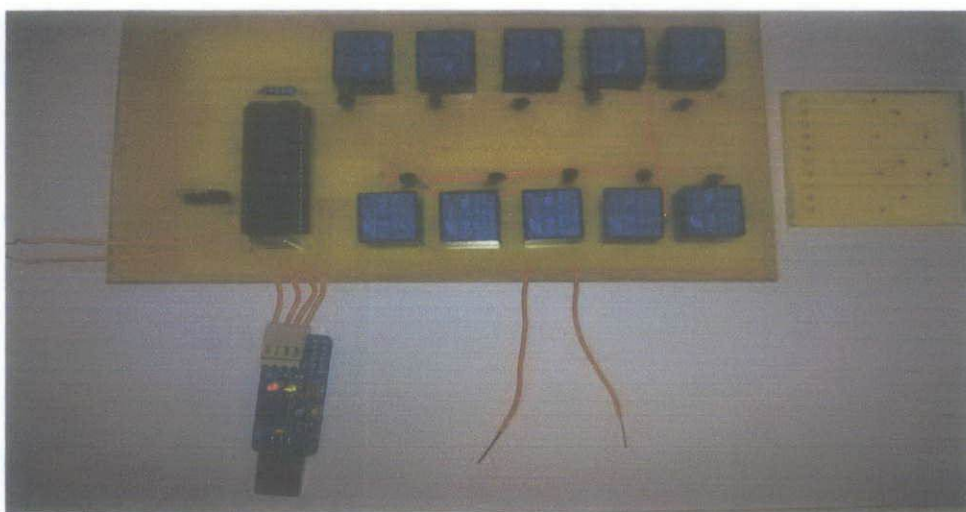


Figure 23: Real external circuit

### 4.3 Corrosion detection capabilities on PCB-based MAS.

#### 4.3.1 First experiment

This experiment is to observe the capabilities of PCB-based MAS in detecting the changes of solution concentration. 3%wt sea salt solution is used as corrosion medium. After 6 days, the concentration of sea salt solution changed to 6%wt and 9%wt of sea salt solution. In addition, it also aims to compare functionality of PCB-based MAS to CMAS probes.

##### 4.3.1.1 Cyanoacrylate Coating PCB-based MAS in Sea Salt Solution.

From figure 24, electrode ten (E10) gave the highest anodic current during these 11 days experiment. Besides, the graph shows the appearance of anodic and cathodic currents. This shows that the PCB-based MAS is working as a same principle like the CMAS probes and it detects the  $I_{corr}$  in the sea salt solution.

From figure 25, anodic currents behaviors are detected from 5 electrodes out of 10 electrodes. The electrodes are E2, E3, E5, E6 and E10. From the maximum corrosion rate equation (equation 8), we can conclude that the maximum anodic current ( $I_{max}^a$ ) is proportional to the maximum corrosion rate ( $CR_{max}$ ). Thus, we can see the trend of increasing and decreasing maximum corrosion rate by observing the  $I_{max}^a$  in the data.

From figure 26, PCB-based MAS can detect the changes of the corrosion solution concentration. On day 1, the maximum corrosion rate is  $\sim 109\mu\text{m}/\text{yr}$  but it slightly increase and decrease from day 2 until day 5. The values vary stably because of the polished copper electrode react actively with the solution and the increase of the corrosion product at the copper electrodes.



On day 6, when the concentration of the sea salt solution changed from 3% to 6% and 9% the drastic changes in the maximum corrosion rate can be seen from  $\sim 127\mu\text{m}/\text{yr}$  to  $\sim 172\mu\text{m}/\text{yr}$ . Maximum corrosion rate increase from day 7 onwards until  $491\mu\text{m}/\text{yr}$  on day 11.

Maximum corrosion rate using the three times of standard deviation of all  $I_{\text{corr}}$  ( $3\sigma$ ) represent the 99% confident in statistics; confident that the measured maximum current is maximum value. This means that  $3\sigma$  of all anodic currents should be near to the maximum anodic current,  $I_{\text{max}}$ . Figure 26, maximum corrosion rate using  $3\sigma$  shows same trend with the graph of maximum anodic current. However, due to the number of electrodes that contain anodic currents, it might vary the maximum corrosion rate of the copper.

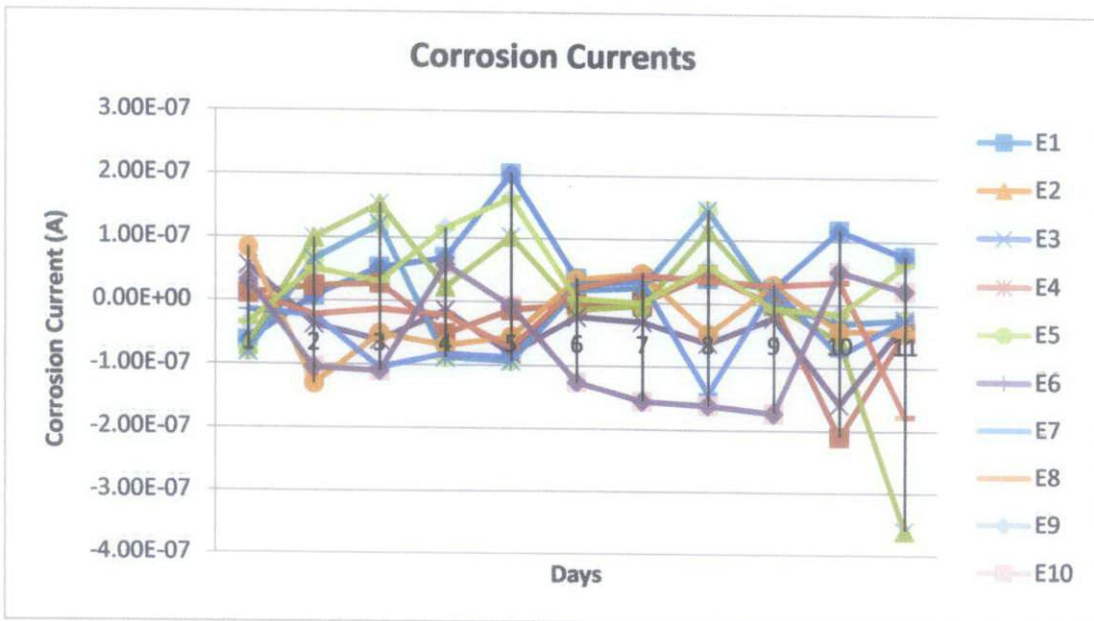


Figure 24: Corrosion current measured for Cyanoacrylate conformal coating in sea salt solution.

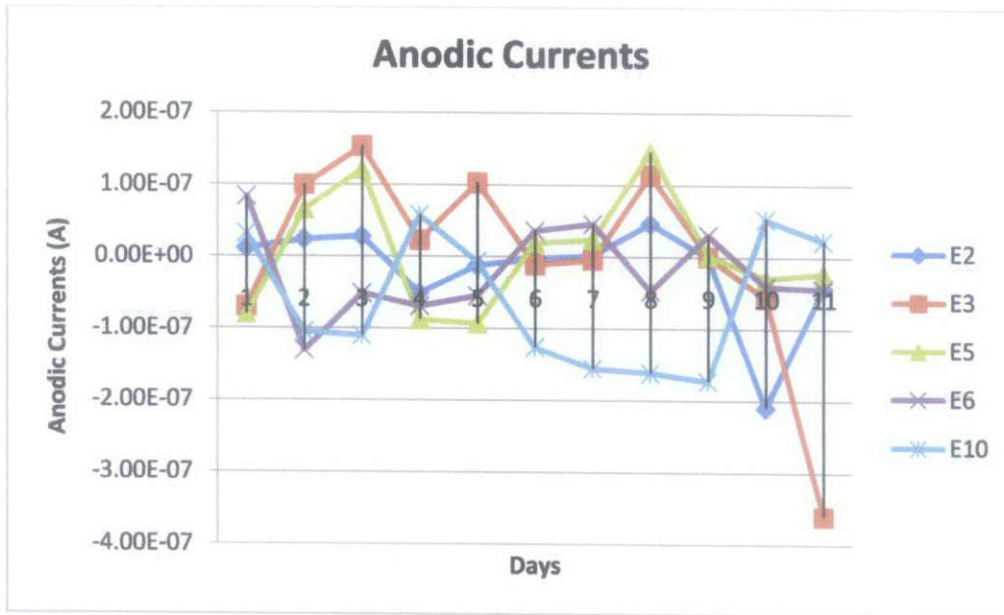


Figure 25: Anodic current for cyanoacrylate conformal coating in sea salt solution

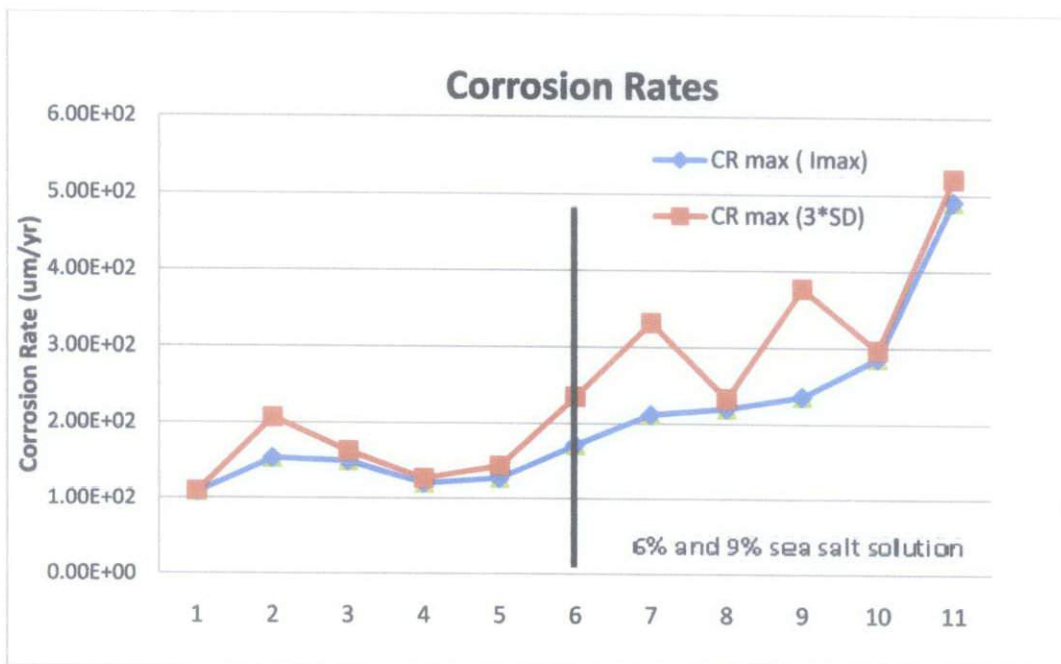


Figure 26: Maximum corrosion rate using high anodic current and 3σ for cyanoacrylate conformal coating in sea salt solution.

#### 4.3.1.2 Epoxy Coating PCB-based MAS in Sea Salt Solution.

From figure 27, the  $I_{corr}$  should nearly in the same range. This is because from Kirchoff current law, the  $I_{corr}$  (anodic and cathodic) should cancel out each other by giving mean of zero. It is ideal case if the mean is zero. In actual case, the  $I_{corr}$  may be diverging a little bit because of the environment effects. However, small divergence of means is acceptable.

From figure 28, anodic currents behavior are detected from 6 electrodes out of 10 electrodes. Those electrodes are E1, E2, E3, E4, E5 and E8. Electrode 2 appear to be dominant in this experiment because four times in producing high anodic current.

In this experiment, it shows that the PCB-based MAS can detect the changes in the concentration of the corrosion solution. This is shown from figure 29 (CRmax for epoxy in sea salt water). The maximum corrosion rates start high at  $\sim 150 \mu\text{m}/\text{yr}$  and drops on day 2 onwards during the 3%wt sea salt solution. This is because when the polished bare copper electrodes touch the corrosive sea salt solution, the corroded vigorously and it maintain in equilibrium because of increasing corrosion product. This value maintainly increase and decrease until day 6 in range of  $\sim 20 \mu\text{m}/\text{yr}$  to  $\sim 56 \mu\text{m}/\text{yr}$ . When concentration 3%wt sea salt solution changed to 6%wt and 9%wt, the sudden increment detected on day 7 from  $\sim 20 \mu\text{m}/\text{yr}$  to  $\sim 67 \mu\text{m}/\text{yr}$ . On day 8 until day 12, the maximum corrosion rates start to decrease back and in stable region between  $\sim 60 \mu\text{m}/\text{yr}$ .

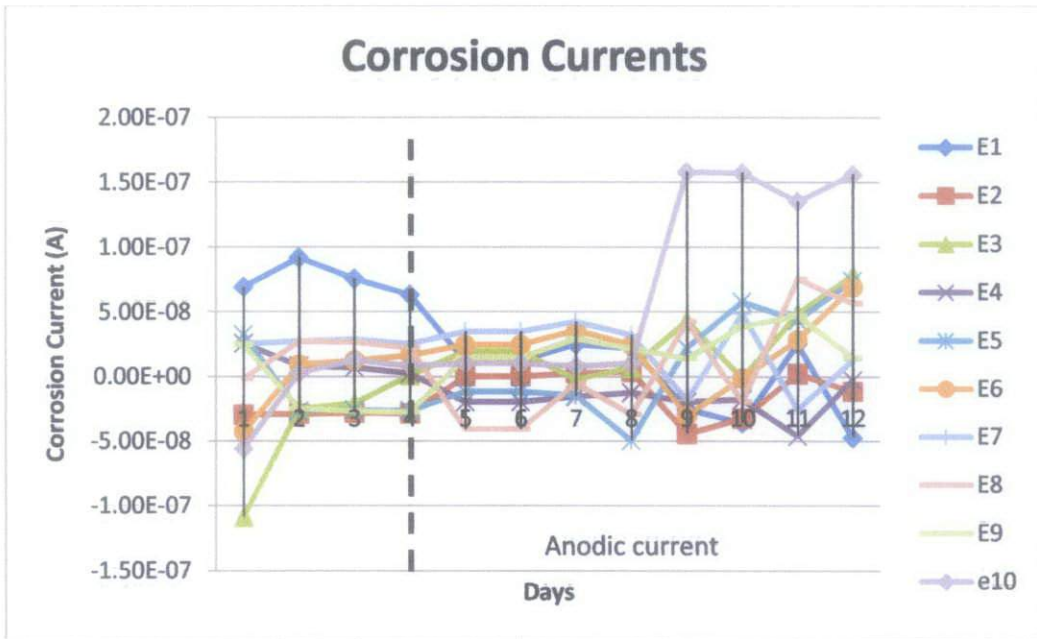


Figure 27: Corrosion current measured for epoxy conformal coating in sea salt solution.

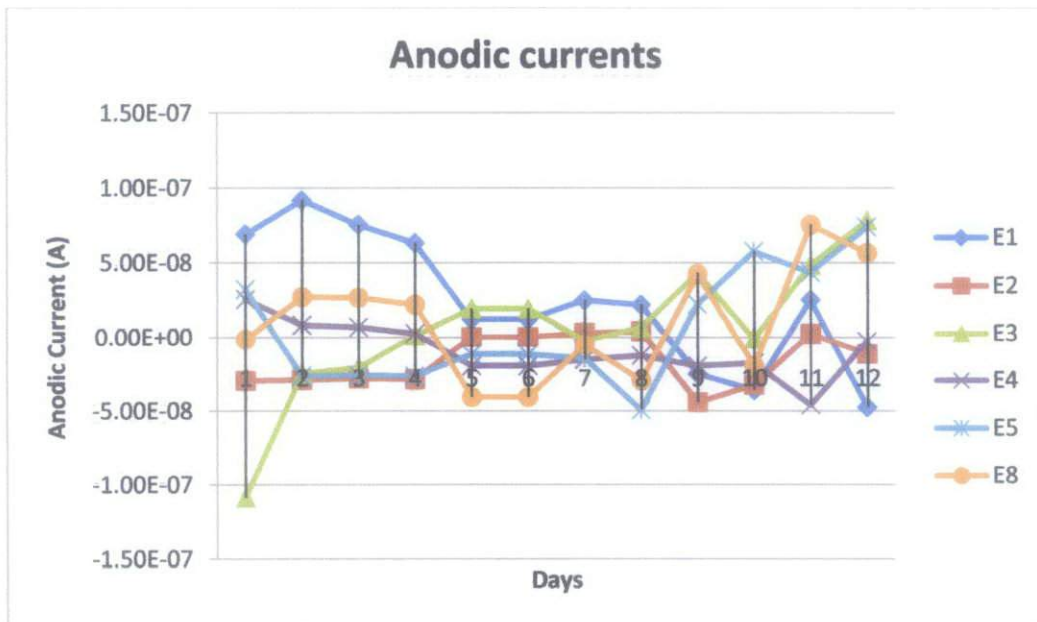


Figure 28: Anodic current for epoxy conformal coating in sea salt solution

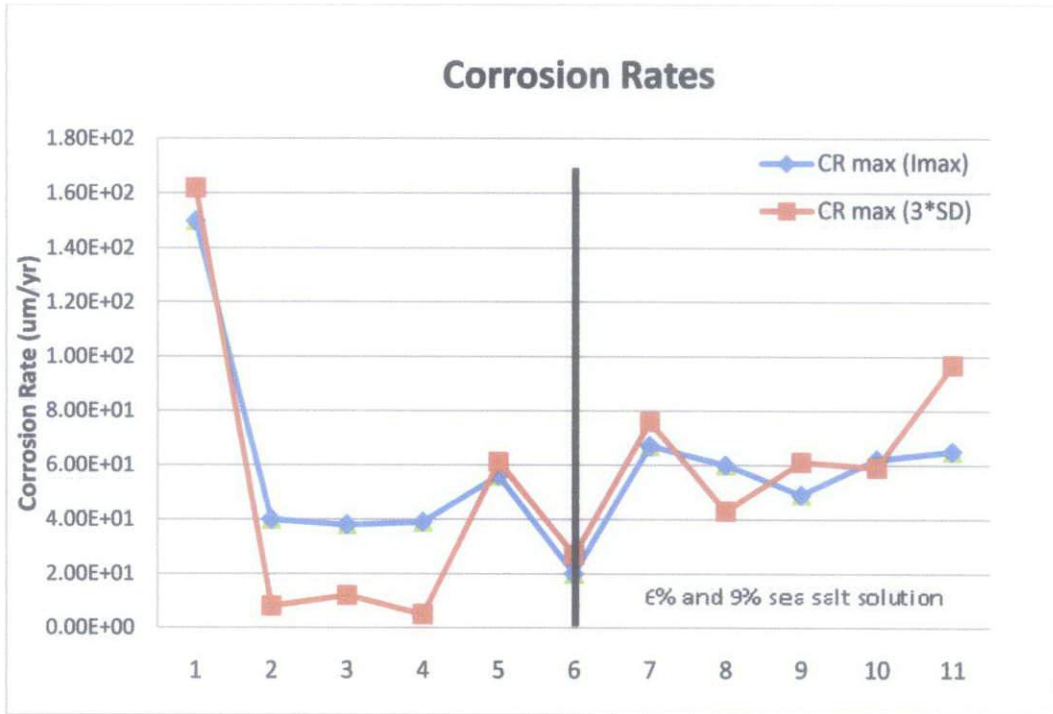


Figure 29: Maximum corrosion rate using high anodic current and  $3\sigma$  for epoxy conformal coating in sea salt solution.

Maximum corrosion rate for cyanoacrylate conformal coating in sea salt solution PCB-based MAS is believed inaccurate. Published data is in range of  $\sim 80\mu\text{m}/\text{yr}$  as shown in figure 30 [14]. PCB-based MAS using cyanoacrylate conformal coating produced maximum corrosion rate around  $\sim 207\mu\text{m}/\text{yr}$ . But, for epoxy conformal coating, the values for maximum corrosion rate is near to the published data which is around  $\sim 60\mu\text{m}/\text{yr}$ . Thus, it is believed to be accurate because small deviation is acceptable.

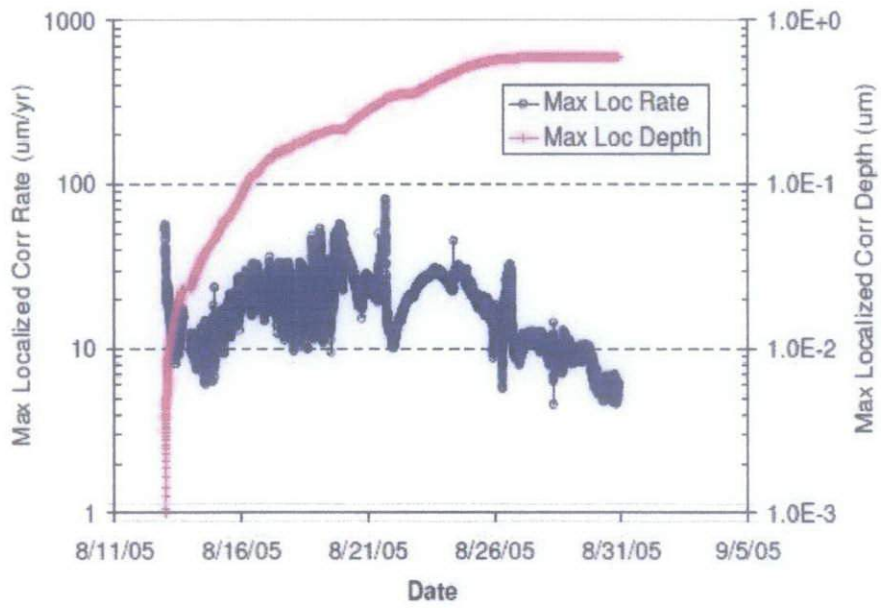


Figure 30: Maximum Localized Maximum corrosion rate and Maximum Localized Depth for Cu in Sea Salt Solution [14].

### 4.3.2 *Second experiment*

Second experiment is to determine the effect of conformal coating on PCB-based MAS performance. The corrosion recognized capability is tested in acidic (HCl) solution with concentration 0.5Mol and 2Mol using cyanoacrylate and epoxy conformal coating as the protection to the copper traces on the sensors from environmental effects.

#### 4.3.2.1 *Cyanoacrylate Conformal Coating in HCl*

Figure 31 shows the  $I_{corr}$  obtained when PCB-based MAS coated with cyanoacrylate immersed in HCl. Electrode 1 (E1) dominated all the anodic currents by producing maximum anodic current in figure 32. In figure 33,  $I_{corr}$  start at  $\sim 24\mu\text{m}/\text{yr}$  and rises drastically in day 3 to  $\sim 1344\mu\text{m}/\text{yr}$  and drop again to  $\sim 463\mu\text{m}/\text{yr}$ . After day 6, the concentration of HCl changed from 0.5Mol to 2Mol. Slight changes in maximum corrosion rates occur in the beginning but high fluctuation of  $I_{corr}$  happened in day 8 with value of  $\sim 3136\mu\text{m}/\text{yr}$ . Maximum corrosion rate remain stable  $\sim 1000\mu\text{m}/\text{yr}$  for the next day.

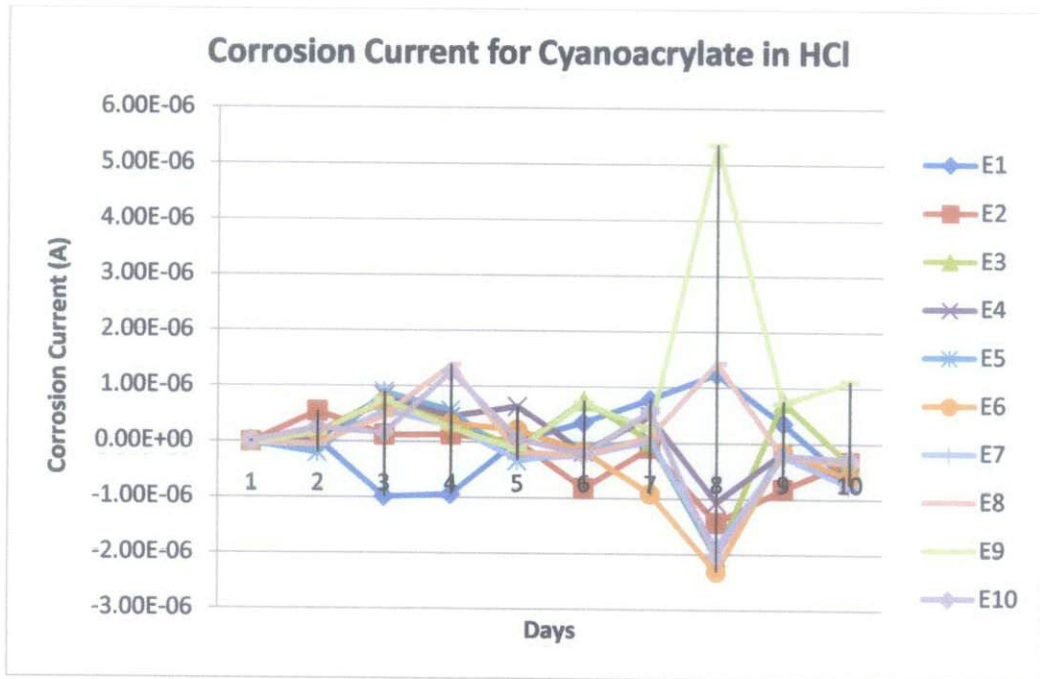


Figure 31: Corrosion current measured for cyanoacrylate conformal coating in HCl.

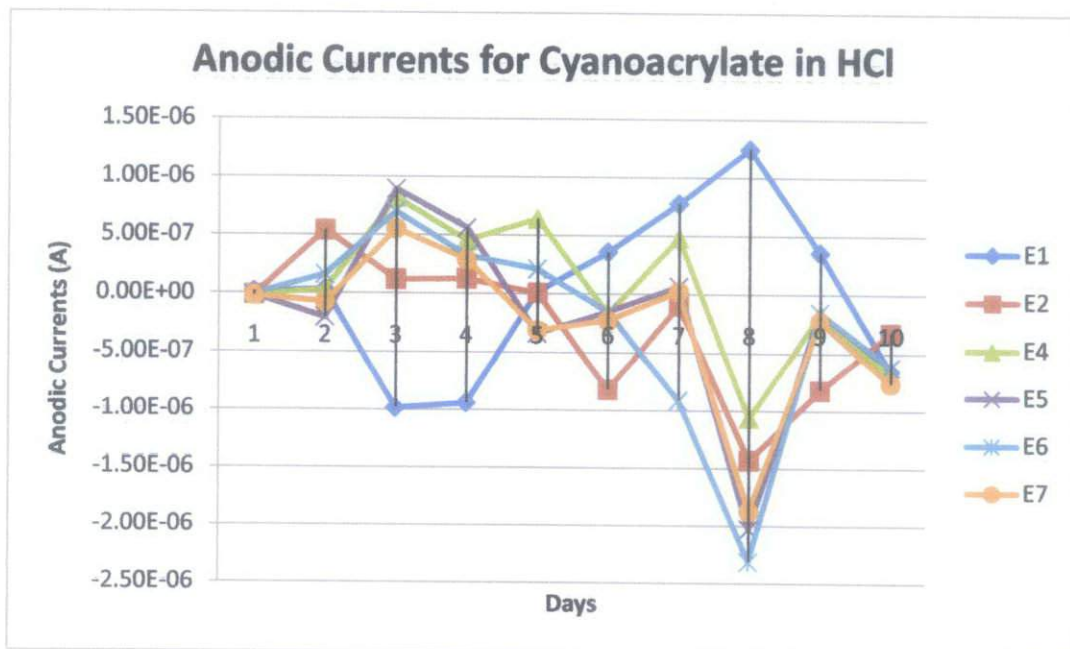


Figure 32: Anodic current for cyanoacrylate conformal coating in HCl



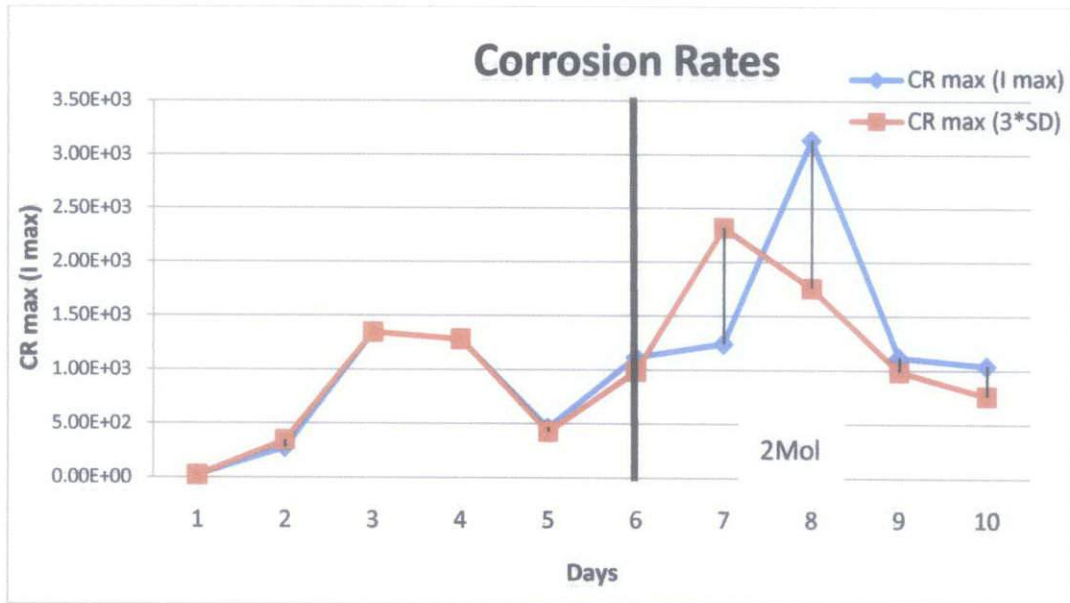


Figure 33: Maximum corrosion rate using high anodic current and  $3\sigma$  for cyanoacrylate conformal coating in HCl.

#### 4.3.2.2 Epoxy Conformal Coating in HCl

Figure 34 shows the  $I_{corr}$  produced when PCB-based MAS coated with epoxy immersed in HCl. Electrode 8 and electrode 10 dominated anodic currents by producing high anodic current in this experiment. From figure 36, it is shown that the maximum corrosion rate of HCl increase from day to day. It starts with  $\sim 859\mu\text{m}/\text{yr}$  and changes drastically in day 3. This is because, the epoxy coated start to peel off from protecting the traces on day 3. When size of peel of start to increase, we can see that the value of  $I_{corr}$  in this experiment get higher. On day 6, when the concentration of HCl changed from 0.5Mol to 2Mol the maximum corrosion rate increase vigorously on day 8 because the peel off of epoxy increase. Maximum corrosion rate end in high value which is  $\sim 39543\mu\text{m}/\text{yr}$ .

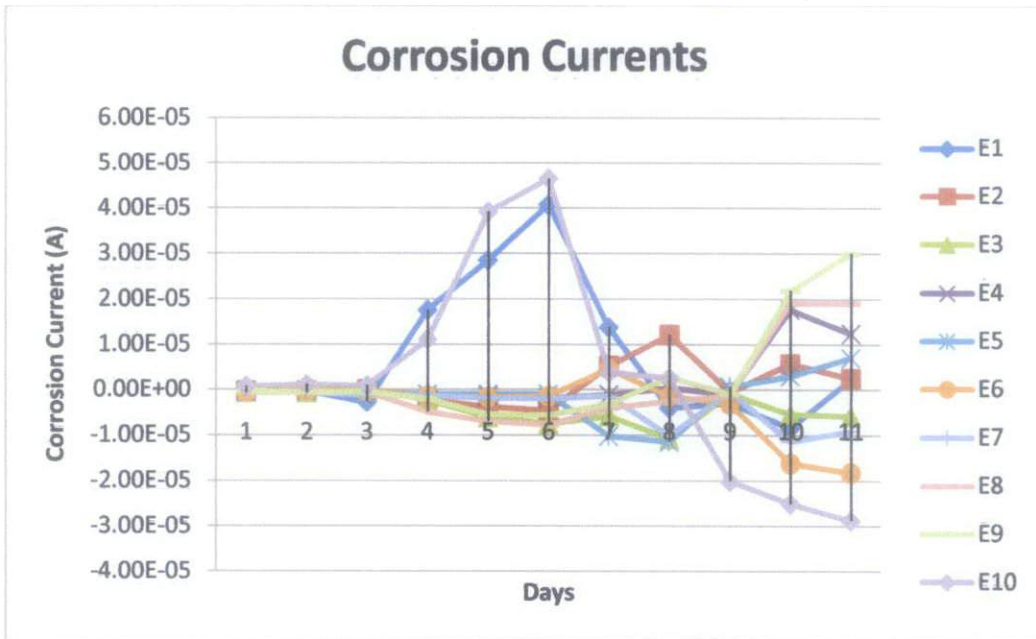


Figure 34: Corrosion current measured for epoxy conformal coating in HCl.

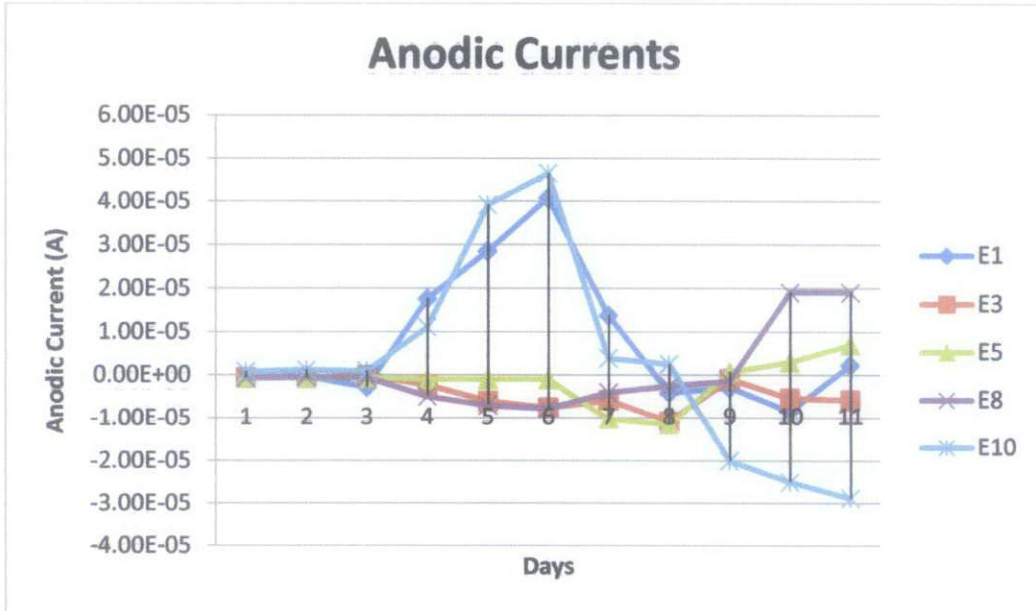


Figure 35: Anodic current for epoxy conformal coating in HCl

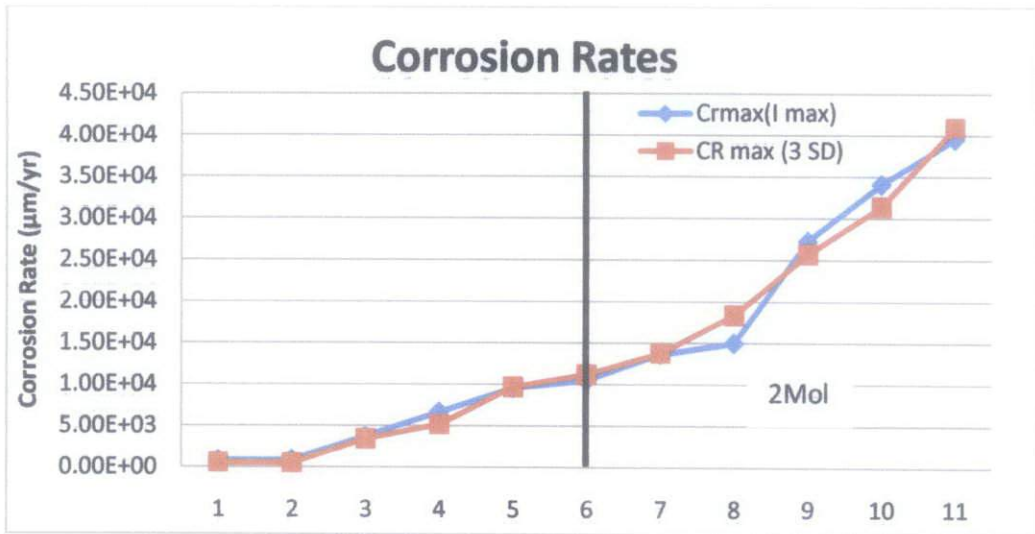


Figure 36: Maximum corrosion rate using high anodic current and  $3\sigma$  for epoxy conformal coating in HCl.

#### 4.3.3 Comparison of two conformal coating

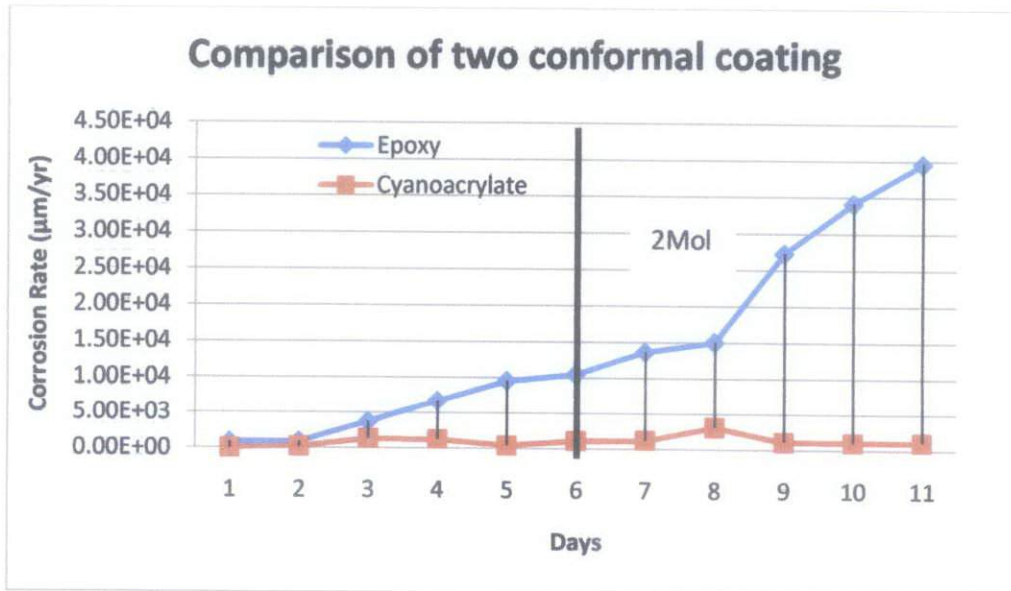


Figure 37: Comparison maximum corrosion rate using  $I_{max}^a$  for two conformal coating PCB-based MAS in HCl solution.

On day 1, maximum corrosion rate for cyanoacrylate is  $\sim 24 \mu\text{m}/\text{yr}$  below than epoxy which is  $\sim 859 \mu\text{m}/\text{yr}$ . this result suggested that cyanoacrylate inhibiting corrosion. On Day 3, when the epoxy start to peel off, the maximum corrosion rate for epoxy rise in sudden to  $\sim 3753 \mu\text{m}/\text{yr}$  compare to the cyanoacrylate which is still rise slightly to  $\sim 1344 \mu\text{m}/\text{yr}$ . when the concentration of HCl change from 0.5Mol to 2.0Mol, the maximum corrosion rate for epoxy increase higher due to peel off the conformal coating in more harsh corrosion environment. However, cyanoacrylate steadily inhibited corrosion after day 6, although there are increments in maximum corrosion rate from the changes of concentration of HCl. Although cyanoacrylate and epoxy which are good insulators for PCB-based MAS, figure 37 shows that the lifetime of PCB-based MAS coated by cyanoacrylate is higher than coated by epoxy due to the inhibit property of the coating.

4.3.4 *Comparison of PCB-based MAS and EIS maximum corrosion rate.*

Electrochemical impedance Spectroscopy (EIS) is an electrochemical technique to measure the corrosion parameters. EIS is a powerful and accurate method to monitor maximum corrosion rate. In this experiment, EIS was used to obtain maximum corrosion rate for FR486 UV copper in the same concentration of HCl which PCB-based MAS was tested [5].

Table 5: Comparison of PCB-based MAS and EIS maximum corrosion rates.

Solution	Concentration	Cyanoacrylate CRmax( $\mu\text{m}/\text{yr}$ )	Epoxy CRmax( $\mu\text{m}/\text{yr}$ )	EIS CRmax( $\mu\text{m}/\text{yr}$ )
HCl	0.5M	~751	~5375	1213
	2M	~1528	~25900	5937

Range of the maximum corrosion rates increase when concentration of the HCl solution increases. Cyanoacrylate have low maximum corrosion rate that indicates that it has inhibit property. As discussed previously, epoxy could not stand harsh corrosive solution and the peel off epoxy will cause very high maximum corrosion rate. Thus, these two conformal coating on PCB-based MAS has high different maximum corrosion rate compare to the EIS corrosion rate due to acceptable reason that being explain previously.

## **CHAPTER 5**

### **CONCLUSION AND RECOMMENDATION**

#### **5.1 Conclusion**

Automated switching external circuit is developed to conduct the maximum corrosion rate monitoring using PCB-based MAS. Automatic switching eases the corrosion monitoring measurement technique. The measurement corrosion current value is valid as the previous manual method because this device can detect anodic and cathodic currents during the experiment. Besides uses of relay did not affected the reading of  $I_{corr}$  because the is nearly 0 Ohm resistivity at relay when it is turn ON during decoupling period. External circuit mainly enhances in term of the working procedures to collect the data of  $I_{corr}$  during the experiment.

First experiment, PCB-based MAS covered with cyanoacrylate and epoxy was immersed in 3%wt, 6%wt and 9%wt sea salt solution. The objective is to observe the detection capability of it when the concentration of corrosive solution changed. Cyanoacrylate conformal coating produced maximum corrosion rate around  $\sim 207\mu\text{m}/\text{yr}$ . But, for epoxy conformal coating, the values for maximum corrosion rate is near to the published data ( $\sim 80\mu\text{m}/\text{yr}$ .) which is around  $\sim 60\mu\text{m}/\text{yr}$ . Thus, it is believed to be accurate.

Second experiment, PCB-based MAS covered with cyanoacrylate and epoxy was immersed in 0.5Mol and 2Mol of HCl. Compare to EIS experiment, cyanoacrylate have low maximum corrosion rate that indicates that it has inhibit property. As discussed previously, epoxy could not stand harsh corrosive solution and the peel off epoxy will cause very high maximum corrosion rate.

## **5.2 Recommendation**

Enhancement of automated switching circuit such as communication between computer and Keithley 6487 Picoammeter using other triggering devices is suggested. There are some other methods to automated the measurement of corrosion monitoring such as using LabView DAQ devices, external triggering to the picoammeter using triggering cable and SCPI programming [16]. When the communication between excelLINUX and Keithley 6487 Picoammeter are established, field experiment such as PCB-based MAS exposed in real corrosive environment can be done for a longer time of period to monitor the maximum corrosion rate for it in high density of rate measurement. Thus, the small changes in the corrosion rates can be analyze well in the future.

## REFERENCES

- [1] Naval Facilities Engineering Command, "Corrosion Control," NAV FAC MO-307, September 1992.
- [2] J.C. Scully, "The Fundamental of Corrosion," Pergamon Press, Third Edition, 2002.
- [3] Pierre R. Roberge, Corrosion Inspection and Monitoring, Wiley Inter-Science, pp.48, 2007
- [4] Pipeline Accident Report, "Natural Gas Pipeline Rupture and Fire Near Carlsberg, New Mexico August 19, 2000". National Transportation Safety Board, Washington DC.
- [5] Aysha Salman, "PCB-Based Planar Multielectrode-Array-Sensor for Corrosion Monitoring", Thesis Master of Science, July 2010.
- [6] Pierre R. Roberge, Corrosion Engineering: Principles and Practices, Mc Graw Hill, 2008.
- [7] Pierre R. Roberge, Corrosion Inspection and Monitoring, Wiley Inter-Science, pp.191- 192, 2007.
- [8] L. Yang, Techniques for corrosion monitoring, Woodhead Publishing, 2008.
- [9] Principle of Coupled Multielectrode Sensor Analyzers from <http://corrinstruments.com> on October 20, 2010, 8:15pm.
- [10] J. Varteresian, Fabricating Printed Circuit Boards, Newnes, 2002.



- [11] Robert L. Boylestad and Louis Nashelsky, *Electronic Devices and Circuit Theory*, Pearson Prentice Hall, 2006.
- [12] L. Yang and X. Sun, "A Method to Reduce the Internal Current Effect on Localized Corrosion Measurement with Coupled Multielectrode Array Sensor," *Corrosion/2008*, paper no. 08395, NACE International 2008.
- [13] L. Yang, N. Sridhar, and D.S. Dunn, "An In-Situ Galvanically Coupled Multielectrode Array Sensor for Localized Corrosion," *Corrosion*, vol.58, pp.1004-1014, 2002.
- [14] X. Sun and L. Yang, "Real-Time Monitoring of Localized and General Corrosion Rates in Simulated Marine Environments Using Coupled Multielectrode Array Sensors," *Corrosion/2006*, paper no. 06679 NACE International 2006.
- [15] Cytron Technologies, "Cytron USB to UART Converter," *User Manual v1.1*, August 2009.
- [16] Keithley Instruments Inc., "Model 6487 Picoammeter/Voltage Source," *References Manual*, November 2002.

## APPENDIX A

Gantt Chart for Final Year Project 1

No.	Detail/ Week	1	2	3	4	5	6	7	8	9	10	11	12	13	14
	<b>FYP 1</b>														
1	Selection Of Project Topic														
2	Preliminary Research Work Corrosion Monitoring Techniques														
3	PCB-based MAS Sensors														
4	Designing Switching Circuit Design														
5	Testing Switching Circuit														
7	Equipment Determination														

## APPENDIX B

Gantt Chart for Final Year Project 2

No.	Detail/ Week	1	2	3	4	5	6	7	8	9	10	11	12	13	14
	<b>FYP 2</b>														
1	PCB circuit design & fabricate														
2	Automated circuit programming (PIC Microcontroller-exceLINX)														
3	Corrosion Rate Monitoring														
4	PCB based MAS with conformal coating														
5	Data Analysis														

## Appendix C

### Microcontroller 18F Coding

```
#include <18F4620.h>
##fuses
HS,NOWDT,NOPROTECT,NOLVP,NOP
UT,NOBROWNOUT //16f
#fuses      INTRC_IO,      NOWDT,
NOPROTECT, NOBROWNOUT, PUT,
NOLVP //18f
#use delay(clock=8000000)
#define time1 30000

//=====
void fungsisatu ();

void main()
{
    fungsisatu ();
}

void fungsisatu ()
{
    //relay
    output_high(pin_b7);
    output_low (pin_b6);
    output_low (pin_b5);
    output_low (pin_b4);
    output_low (pin_b3);
    output_low (pin_b2);
    output_low (pin_b1);
    output_low (pin_b0);
    output_low (pin_d7);
    output_low (pin_d6);
    //led
    output_high(pin_a0);
    output_low (pin_a1);
    output_low (pin_a2);
    output_low (pin_a3);
    output_low (pin_a4);
    output_low (pin_a5);
    output_low (pin_e0);
    output_low (pin_e1);
    output_low (pin_e2);
    output_low (pin_c0);
    delay_ms(time1);

    //relay
    output_low (pin_b7);
    output_high (pin_b6);
    output_low (pin_b5);

    output_low (pin_b4);
    output_low (pin_b3);
    output_low (pin_b2);
    output_low (pin_b1);
    output_low (pin_b0);
    output_low (pin_d7);
    output_low (pin_d6);
    //led
    output_low (pin_a0);
    output_high (pin_a1);
    output_low (pin_a2);
    output_low (pin_a3);
    output_low (pin_a4);
    output_low (pin_a5);
    output_low (pin_e0);
    output_low (pin_e1);
    output_low (pin_e2);
    output_low (pin_c0);
    delay_ms(time1);

    //relay
    output_low(pin_b7);
    output_low (pin_b6);
    output_high (pin_b5);
    output_high (pin_b4);

```

```
output_low (pin_b3);
output_low (pin_b2);
output_low (pin_b1);
output_low (pin_b0);
output_low (pin_d7);
output_low (pin_d6);
```

```
//led
output_low (pin_a0);
output_low (pin_a1);
output_low (pin_a2);
output_high (pin_a3);
output_low (pin_a4);
output_low (pin_a5);
output_low (pin_e0);
output_low (pin_e1);
output_low (pin_e2);
output_low (pin_c0);
delay_ms(time1);
```

```
//relay
```

```
output_low(pin_b7);
output_low (pin_b6);
output_low (pin_b5);
output_low (pin_b4);
output_high (pin_b3);
output_low (pin_b2);
output_low (pin_b1);
output_low (pin_b0);
output_low (pin_d7);
output_low (pin_d6);
```

```
//led
```

```
output_low (pin_a0);
output_low (pin_a1);
output_low (pin_a2);
output_low (pin_a3);
output_high (pin_a4);
output_low (pin_a5);
output_low (pin_e0);
output_low (pin_e1);
output_low (pin_e2);
output_low (pin_c0);
delay_ms(time1);
```

```
//relay
```

```
output_low(pin_b7);
output_low (pin_b6);
output_low (pin_b5);
output_low (pin_b4);
output_low (pin_b3);
output_high (pin_b2);
output_low (pin_b1);
output_low (pin_b0);
output_low (pin_d7);
output_low (pin_d6);
```

```
//led
```

```
output_low (pin_a0);
output_low (pin_a1);
output_low (pin_a2);
output_low (pin_a3);
output_low (pin_a4);
output_high (pin_a5);
output_low (pin_e0);
output_low (pin_e1);
output_low (pin_e2);
output_low (pin_c0);
delay_ms(time1);
```

```
//relay
```

```
output_low(pin_b7);
output_low (pin_b6);
output_low (pin_b5);
output_low (pin_b4);
output_low (pin_b3);
output_low (pin_b2);
output_high (pin_b1);
output_low (pin_b0);
output_low (pin_d7);
output_low (pin_d6);
```

```
//led
```

```
output_low (pin_a0);
output_low (pin_a1);
output_low (pin_a2);
output_low (pin_a3);
output_low (pin_a4);
output_low (pin_a5);
output_high (pin_e0);
output_low (pin_e1);
output_low (pin_e2);
output_low (pin_c0);
delay_ms(time1);
```

```
//relay
```

```
output_low(pin_b7);
output_low (pin_b6);
output_low (pin_b5);
output_low (pin_b4);
output_low (pin_b3);
output_low (pin_b2);
output_low (pin_b1);
output_high (pin_b0);
output_low (pin_d7);
output_low (pin_d6);
```

```
//led
```

```
output_low (pin_a0);
output_low (pin_a1);
output_low (pin_a2);
output_low (pin_a3);
output_low (pin_a4);
```

```

output_low (pin_a5);
output_low (pin_e0);
output_high (pin_e1);
output_low (pin_e2);
output_low (pin_c0);
delay_ms(time1);

//relay
output_low(pin_b7);
output_low (pin_b6);
output_low (pin_b5);
output_low (pin_b4);
output_low (pin_b3);
output_low (pin_b2);
output_low (pin_b1);
output_low (pin_b0);
output_high(pin_d7);
output_low (pin_d6);
//led
output_low (pin_a0);
output_low (pin_a1);
output_low (pin_a2);
output_low (pin_a3);
output_low (pin_a4);
output_low (pin_a5);
output_low (pin_e0);
output_low (pin_e1);
output_low (pin_e2);
output_high (pin_c0);
delay_ms(time1);
}
output_low (pin_c0);
delay_ms(time1);

//relay
output_low (pin_b7);
output_low (pin_b6);
output_low (pin_b5);
output_low (pin_b4);
output_low (pin_b3);
output_low (pin_b2);
output_low (pin_b1);
output_low (pin_b0);
output_low (pin_d7);
output_high (pin_d6);
//led
output_low (pin_a0);
output_low (pin_a1);
output_low (pin_a2);
output_low (pin_a3);
output_low (pin_a4);
output_low (pin_a5);
output_low (pin_e0);
output_low (pin_e1);
output_low (pin_e2);
output_high (pin_c0);
delay_ms(time1);
}

```